The Kinetic Physics of Magnetotail Dynamics: Reconnection, Ballooning, and Dipolarization Fronts

P.L. Pritchett
UCLA

Collaborators: F.V. Coroniti
Y. Nishimura

Outline

- Introduction to magnetotail and PIC simulations
- Effect of B_z in stabilizing spontaneous tearing instability
- Observational guidance
- Possible role of ballooning/interchange instability
  - Generates fronts with ion kinetic scale thickness and ~ R_E east-west extent
  - Generates intense off-axis waves ahead of fronts
  - Leads to structuring of auroral streamers
- Properties of jet (dipolarization) fronts associated with localized reconnection
- Summary/Questions

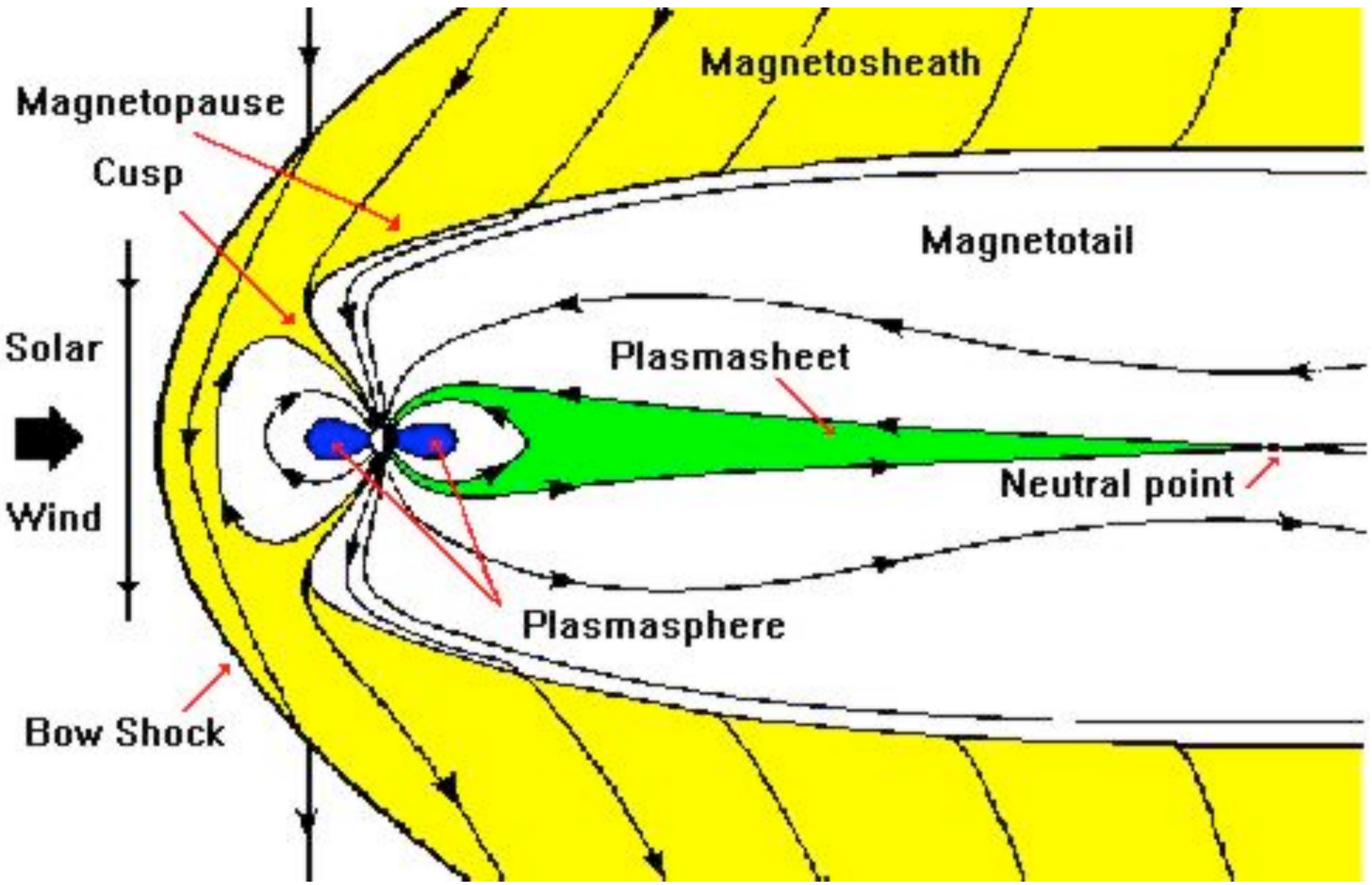

Essential complication in the magnetotail (as opposed to magnetopause) is the presence of a quasi-permanent B_z component of the magnetic field. Field lines generally are never strictly anti-parallel. $B_z \sim 0.1\ B_0$.

Characteristic Parameters

- Proton Cyclotron Frequency in 20 nT field : $\Omega_{i0} = 1.9\ s^{-1}$ ($\Omega_{i0}^{-1} = 0.52$ s)
- Proton Inertial Length at density of 0.3 cm^{-3} : $d_i = c/\omega_{pi} = 416$ km $= R_E/15$
- Proton (5 keV) Gyroradius in 20 nT field: $\rho_{i0} = V_{Ti}/\Omega_{i0} = 520$ km
- Stochasticity Parameter (Büchner & Zelenyi): $\kappa_j = (B_n/B_0)\ (L/\rho_{j0})^{1/2}$

  ~ 0.5 for protons ($L = 2\ R_E$)
  ~ 5 for electrons ($T_e = T_i/5$)

- Curvature Radius $R_c = 1/k_c$, $k_c = n \cdot [(b \cdot \nabla)b] = (1/B_n)(dB_x/dz)$ on axis

Characteristics of (Most) PIC Simulations

PIC simulations follow full dynamics of ions and electrons; must resolve all spatial and temporal scales.

Cost of simulation: In 2D $\propto (M_i/m_e)^2$, In 3D $\propto (M_i/m_e)^{5/2}$

For Harris current sheet equilibrium: $c/V_{Te} = (1 + T_i/T_e)^{(1/2)}\ \omega_{pe}/\Omega_{ce}$

Magnetotail: $T_i/T_e \sim 7$, $\omega_{pe}/\Omega_{ce} \sim 8 - 10$, $c/V_{Te} \sim 25$

Typical PIC Simulation: $T_i/T_e = 4$, $\omega_{pe}/\Omega_{ce} = 2$, $c/V_{Te} = 4.5$

Cost in 2D $\propto (\omega_{pe}/\Omega_{ce})^3$

Cost in 3D $\propto (\omega_{pe}/\Omega_{ce})^4$

Spatial Scales: given in units of c/ω_{pi} (normally)

Velocity: given in units of V_A (or sometimes V_{Ti}), typically ~ 1000 km/s

Reconnection Onset in Presence of B_z

- Usual Reconnection Configuration: Harris Current sheet; not directly applicable to magnetotail due to B_z.

- Electron Tearing Instability: not viable since cyclotron motion removes electron Landau resonance.

- Ion Tearing Instability?
  - Unless half width comparable to d_i, growth rate too small to overcome ion magnetization.
  - Electron stabilization effect: Either electron adiabaticity (Lembège & Pellat, 1982) or simply conservation of P_y in 2D system (Pellat et al., 1991) ensures that tearing mode EM field produces strong compression of electron density. Energy associated with this compression exceeds free energy in reversed B configuration.
  - Condition for electron stabilization: $k\rho_{en} < 1$.

$$k\rho_{en} = kL\,(m_e T_e/M_i T_i)^{1/2}\,(\rho_{i0}/L)(B_0/B_n) < 1$$

0.5   0.010   1 - 0.10

$B_n/B_0 > 0.0005 - 0.005$

$B_n > 0.01 - 0.1$ nT

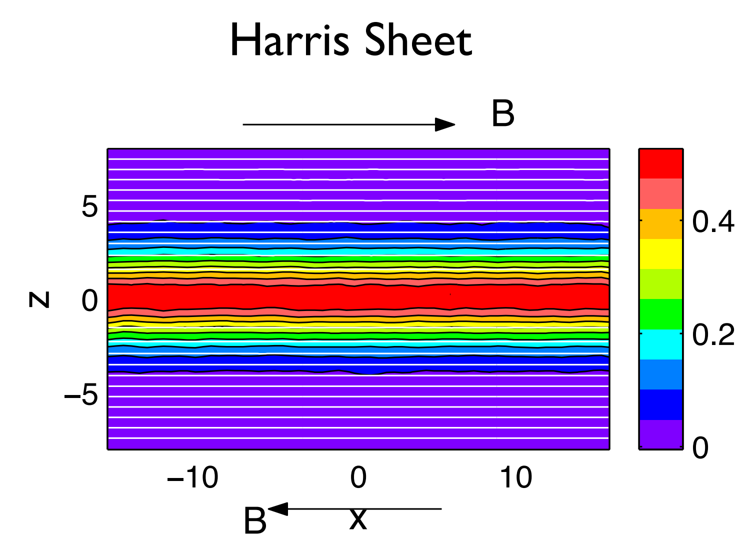

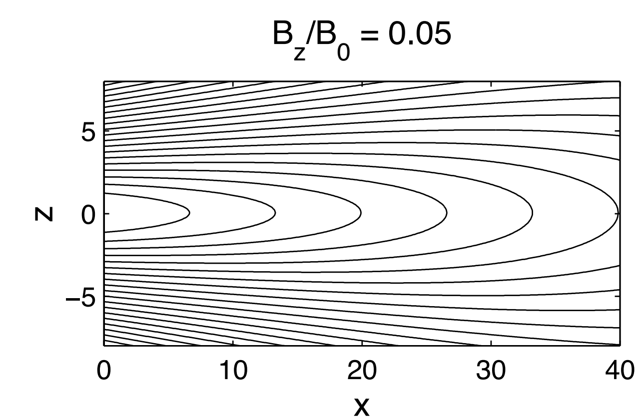

Thus spontaneous tearing instability unlikely to occur in magnetotail

2D PIC Simulations

$k\rho_{en} = 3.7$

$k\rho_{en} = 1.8$

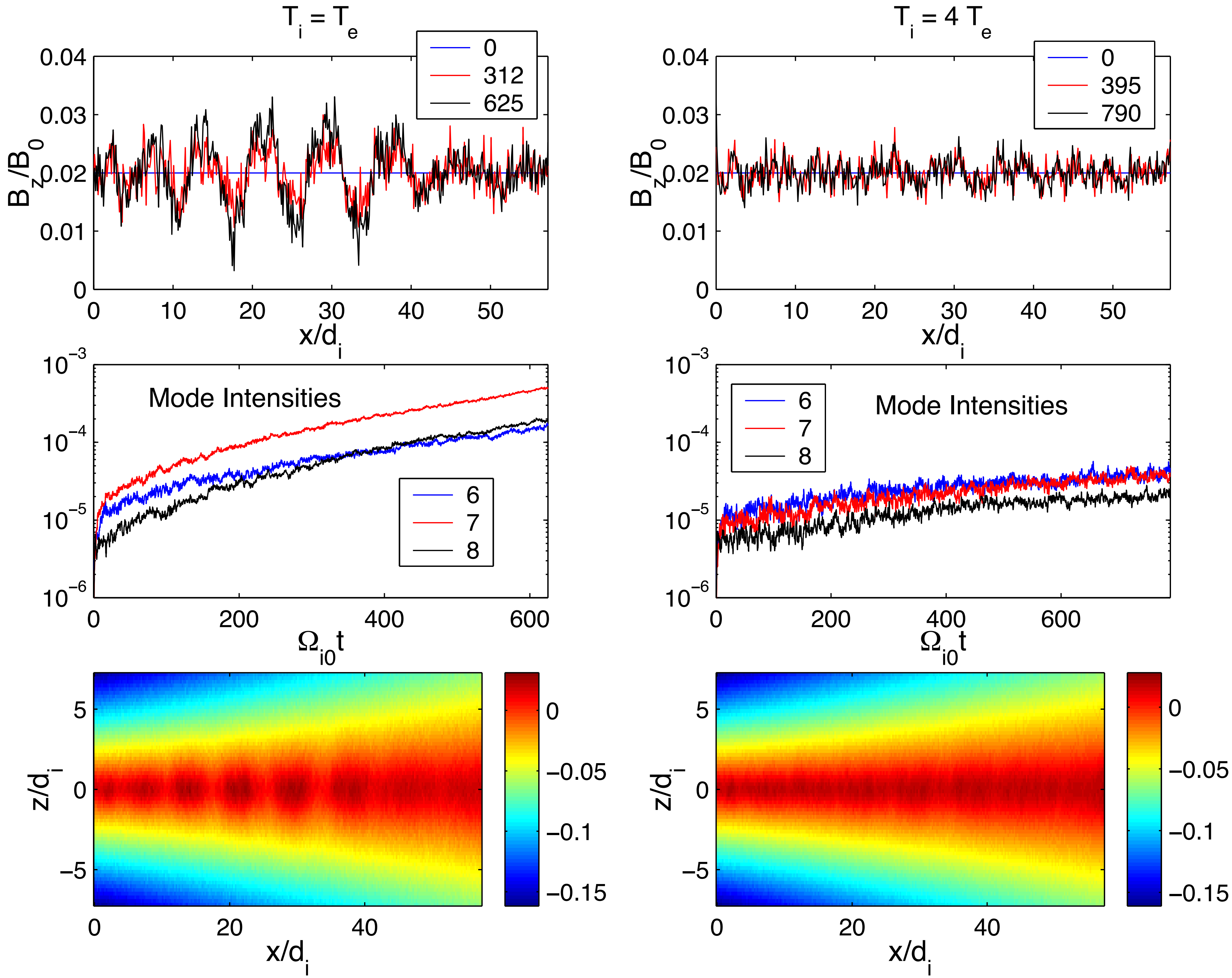

2D x,z simulations: $B_z = 0.02\ B_0$, half-width $L = \rho_{i0}$, $m_i/m_e = 64$, $n_b = 0$

Since Reconnection Clearly Occurs in Magnetotail, What are the Alternatives?

- External Driving: Enhanced convection E_y field arising from southward IMF can force thinning of current sheet and force local reversal of B_z profile [Pritchett and Coroniti, 1995, 1997; Hesse and Schindler, 2001].

- Direct day-night coupling [Nishimura et al., 2014]: dayside flow channel and PMAF followed by polar cap airglow patch that crosses the polar cap followed by nightside PBIs and plasma sheet flow bursts.

- Turbulence in the Tail: local reversals of B_z might arise randomly from tail variability.

- Sitnov & Schindler (2010): May be able to circumvent electron stabilization for equilibria with more than 2 characteristic spatial scales ("hump" configuration).

- Non-Reconnection processes: Role of bubbles in the magnetotail [Pontius and Wolf, 1990; Chen and Wolf, 1993]. Once produced, bubbles should propagate earthward due to buoyancy effect, perhaps explaining formation of fronts in near-Earth plasma sheet.

Plasma Sheet

- Curved magnetic geometry (finite B normal) can have significant effects on particle dynamics for both electrons and ions: bounce and drift resonant interactions.
- Must use (at least) 2D equilibrium to describe tail current sheet.
- Mid-tail minima in B_z are observed during periods of extended magnetospheric convection (Sergeev et al., 1994) and expected from MHD models (Hau et al., 1989).
- B_z minimum also observed by Saito et al. [2010] (THEMIS) at ~ 10 R_E: persists for 20 minutes.

Sergeev et al., 1994

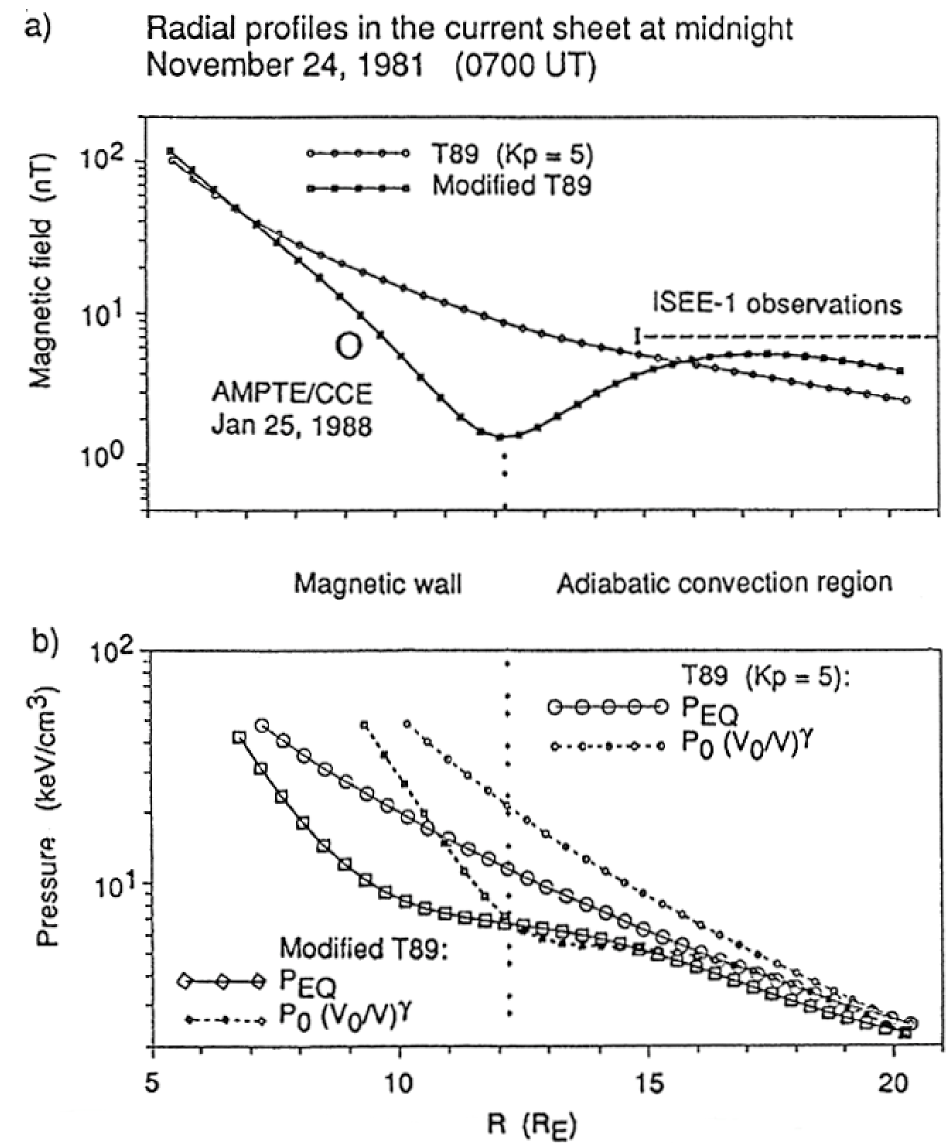

Plasma Sheet Onset Conditions

Saito et al. [2010]: THEMIS observations on April 8 & 12, 2009.

- Infer B_z minimum at 10 R_E, persists for 20 min prior to breakup
- Equatorial B_z as small as 1 nT

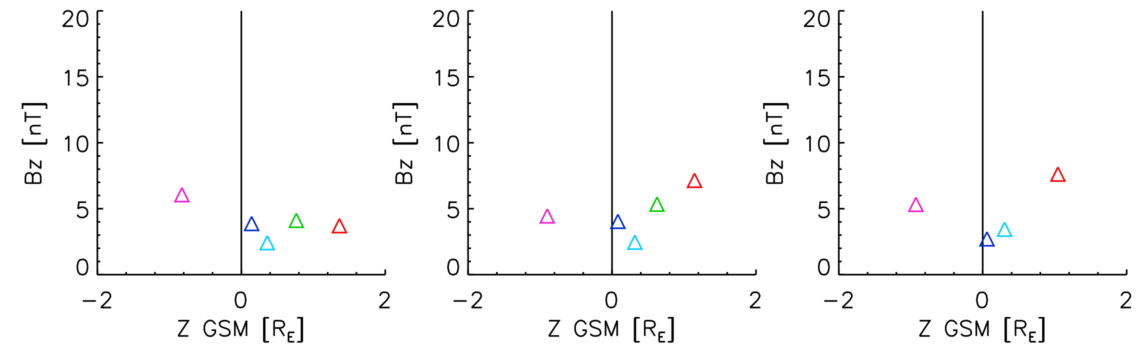

-1 hr

-20 m

-3 m

Machida et al. [2009]: Statistical study of temporal and spatial development of near-Earth magnetotail around substorm onset using Geotail data.

Observe enhanced B_z around -20R_E with a minimum earthward at ~-18R_E; tailward of max B_z decreases, suggesting a possible hump structure.

B_z

t (min)

-6

0

4

|z|

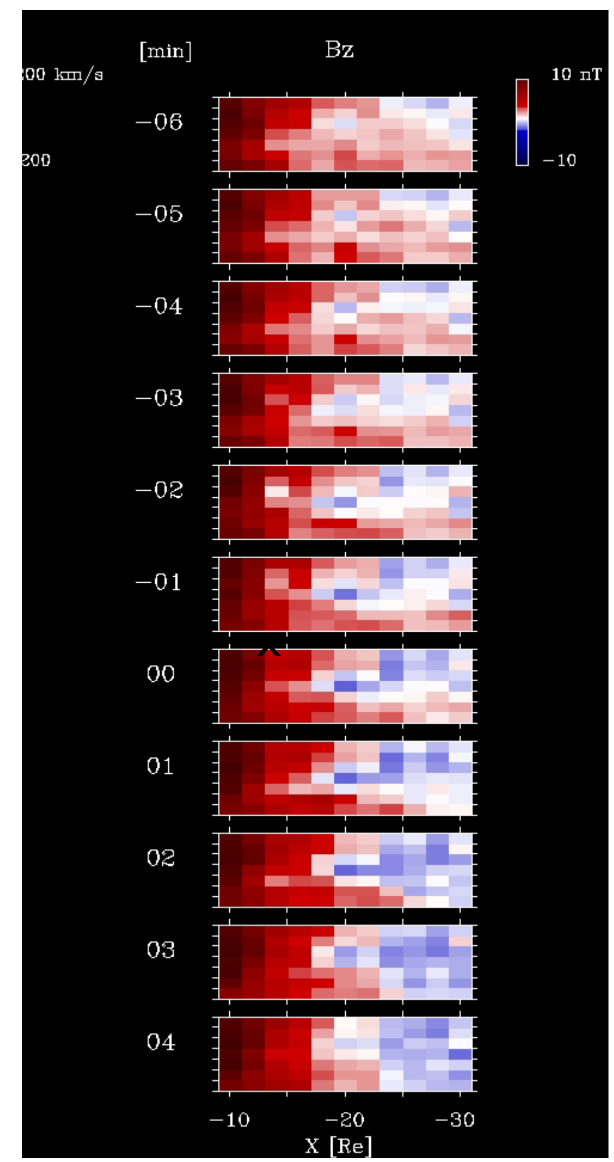

Simulation Model

- 3D Particle-in-Cell
- 2D Current sheet equilibrium in x,z with minimum in equatorial B_z field
- Electrons are adiabatic in right half of tailward gradient B_z region
- $m_i/m_e = 64$, $L/\rho_{i0} = 1.6$, $\rho_{i0} = 16\ \Delta$, 512 X 1024 X 256 grid
- Lobe field = $2.4B_0$ at $x = 192 \Rightarrow B_0 \approx 12$ nT;

  equatorial $\beta \sim 600$
- Boundary conditions:

  x: closed, $\delta E_y = 0$, particles reflected
  into opposite half z plane

  y: periodic

  z: conducting

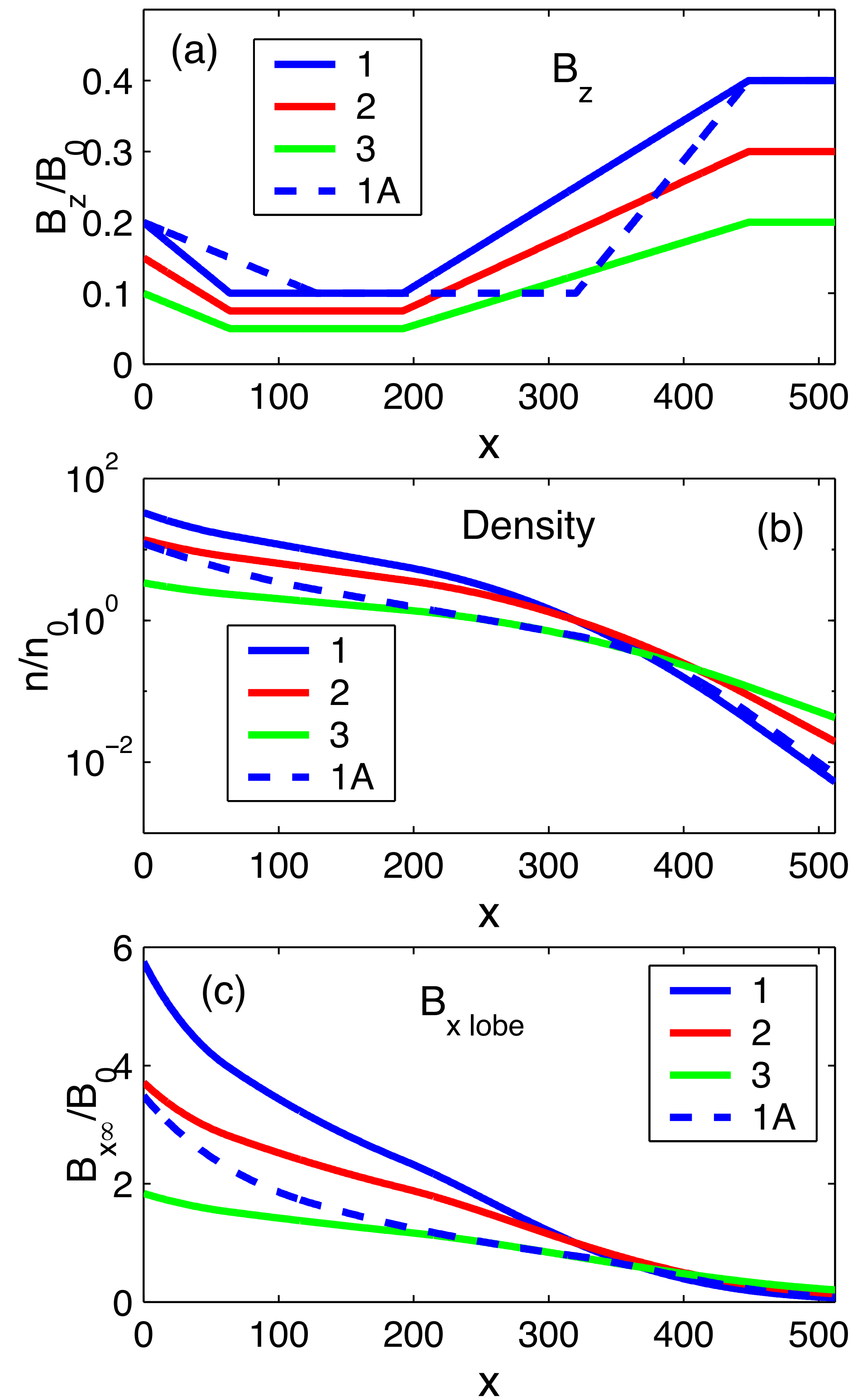

Bubbles and the Entropy Profile

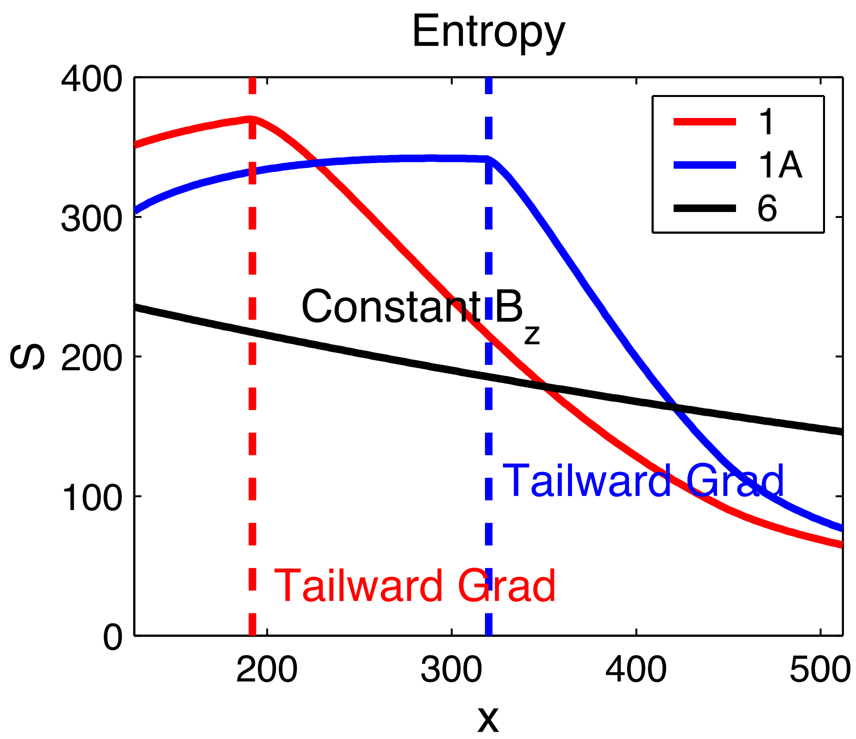

It has long been speculated that small, isolated density depletions ("bubbles") could form in the mid- or distant tail and propagate earthward due to buoyancy (Pontius and Wolf, 1990; Chen and Wolf, 1993).

The behavior of bubbles has been shown to be closely connected to the variation of the entropy as a function of distance down the tail (Birn et al., 2004).

MHD Interchange Instability:

- Hurricane et al. (1996) showed that the Lembege-Pellat (constant B_z) profile is unstable.
- Maltsev & Mingalev (2000) showed criterion is satisfied for an increasing B_z if $dV/dr < 0$, where $V = \int dl/B$ is the flux tube volume.
- More generally, tail-like equilibria are stable (unstable) when the entropy S increases (decreases) with distance down the tail (Schindler & Birn, 2004).

The present equilibria have a decreasing entropy profile in the region of the tailward gradient in B_z and thus are likely to be unstable.

Alternative interpretation: The tailward gradient region in B_z could also represent the leading edge of a reconnection front viewed in the rest frame of the front.

2D simulation of a Harris sheet driven by a finite duration E_y driving field peaked at x = 0 produces an X line with fronts propagating both earthward and tailward.

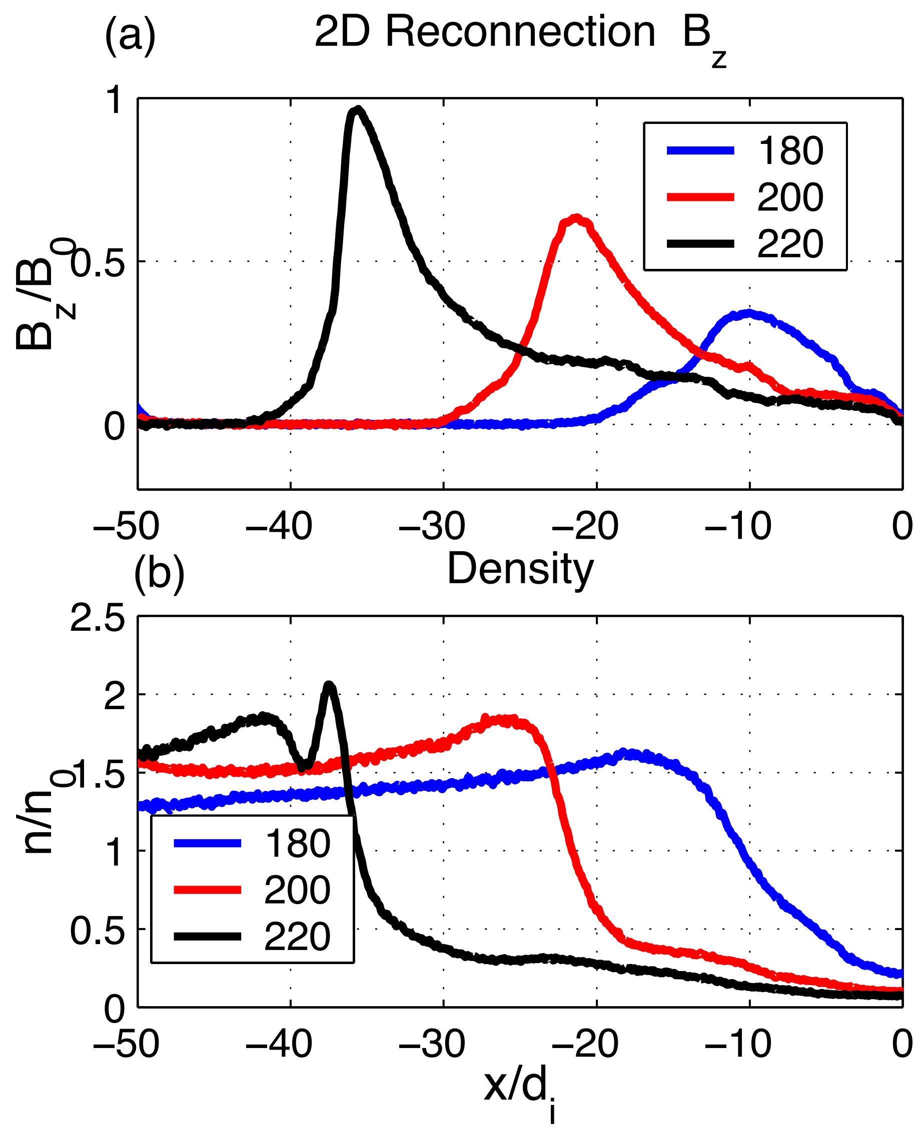

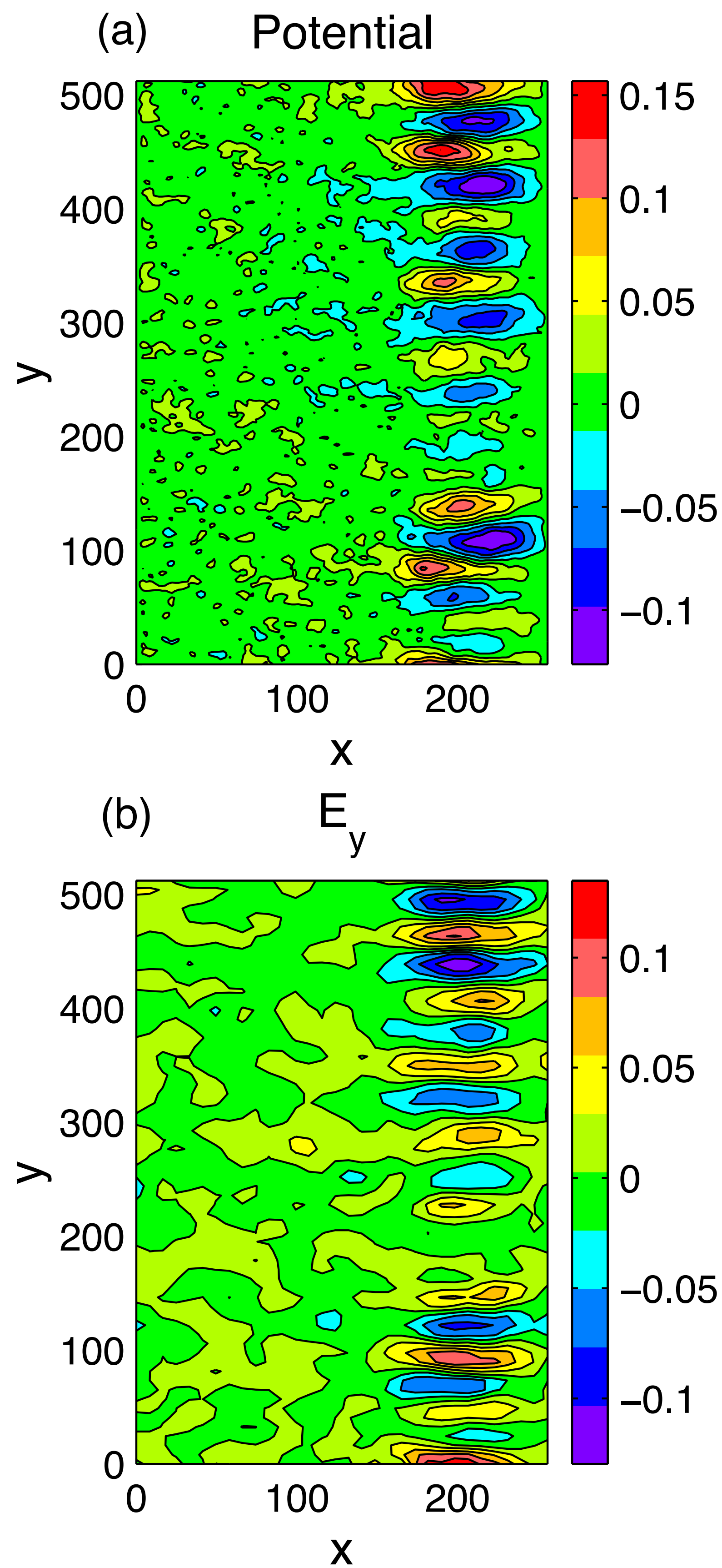

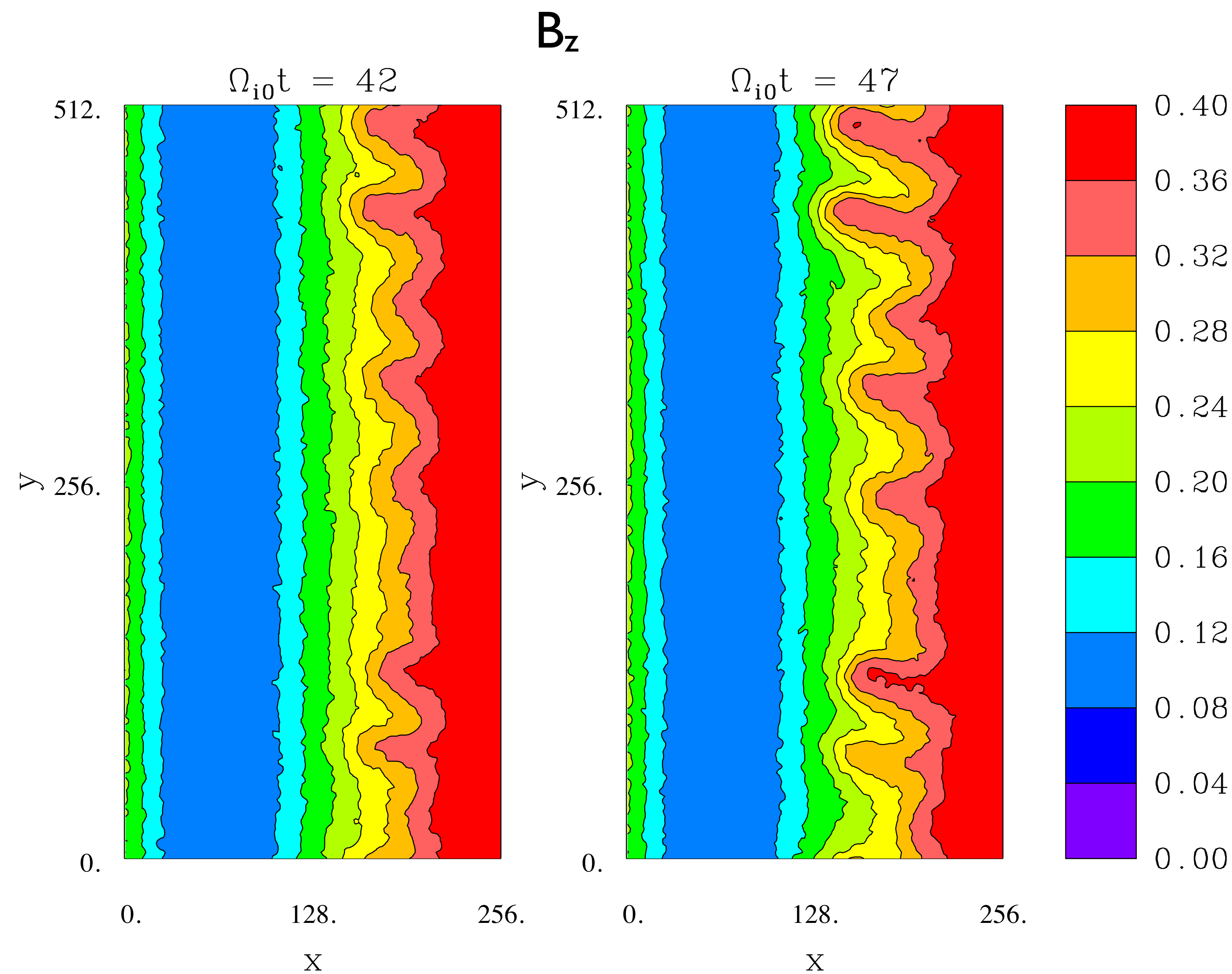

Mode structures develop in right half of tailward gradient region where electrons are adiabatic. Equatorial plane structure has character of an interchange mode.

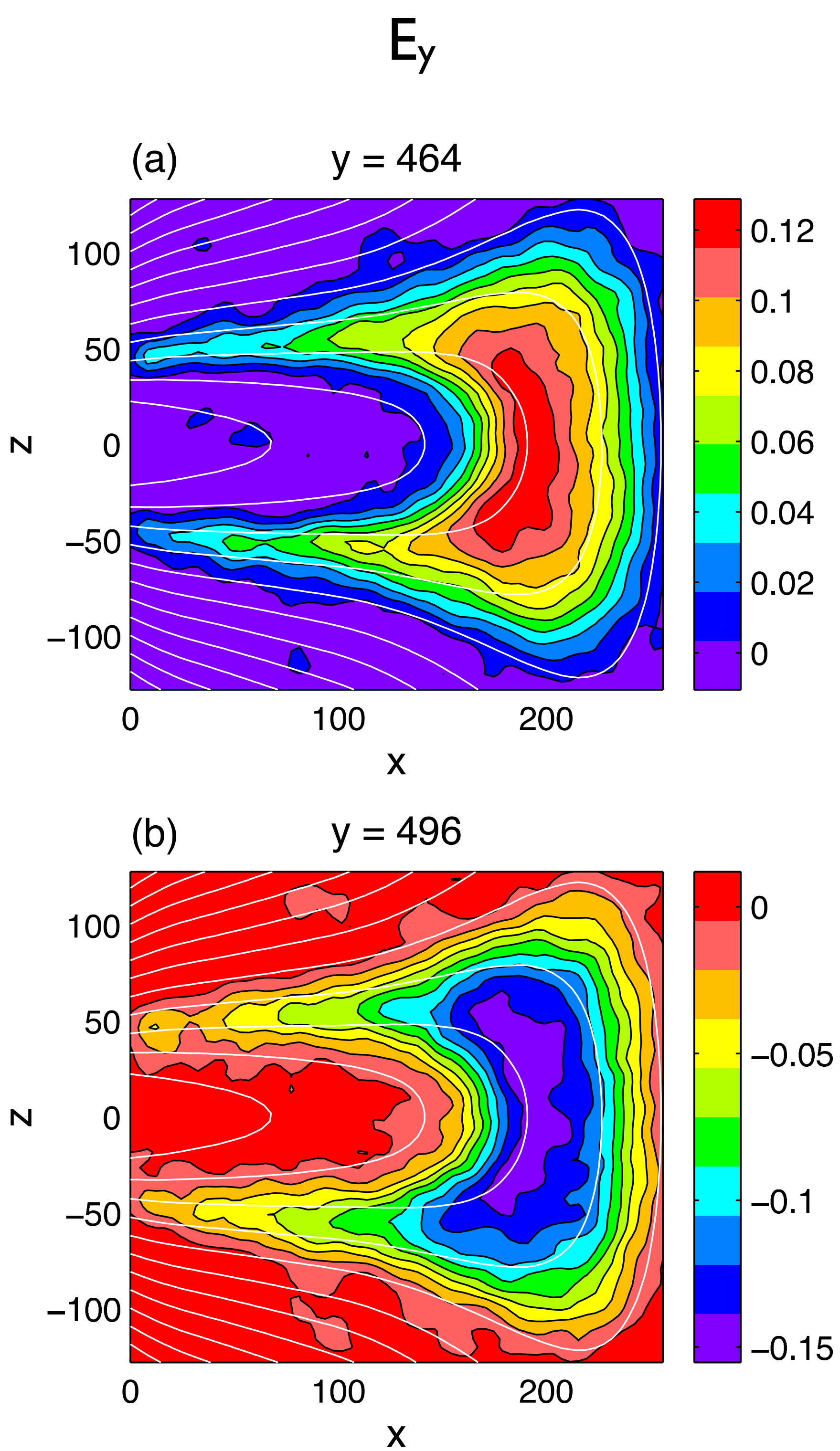

Mode structures also extend along field lines earthward toward ionosphere.

Unlike MHD interchange modes, there is large perturbation resulting from the finite $E_{||}$ field.

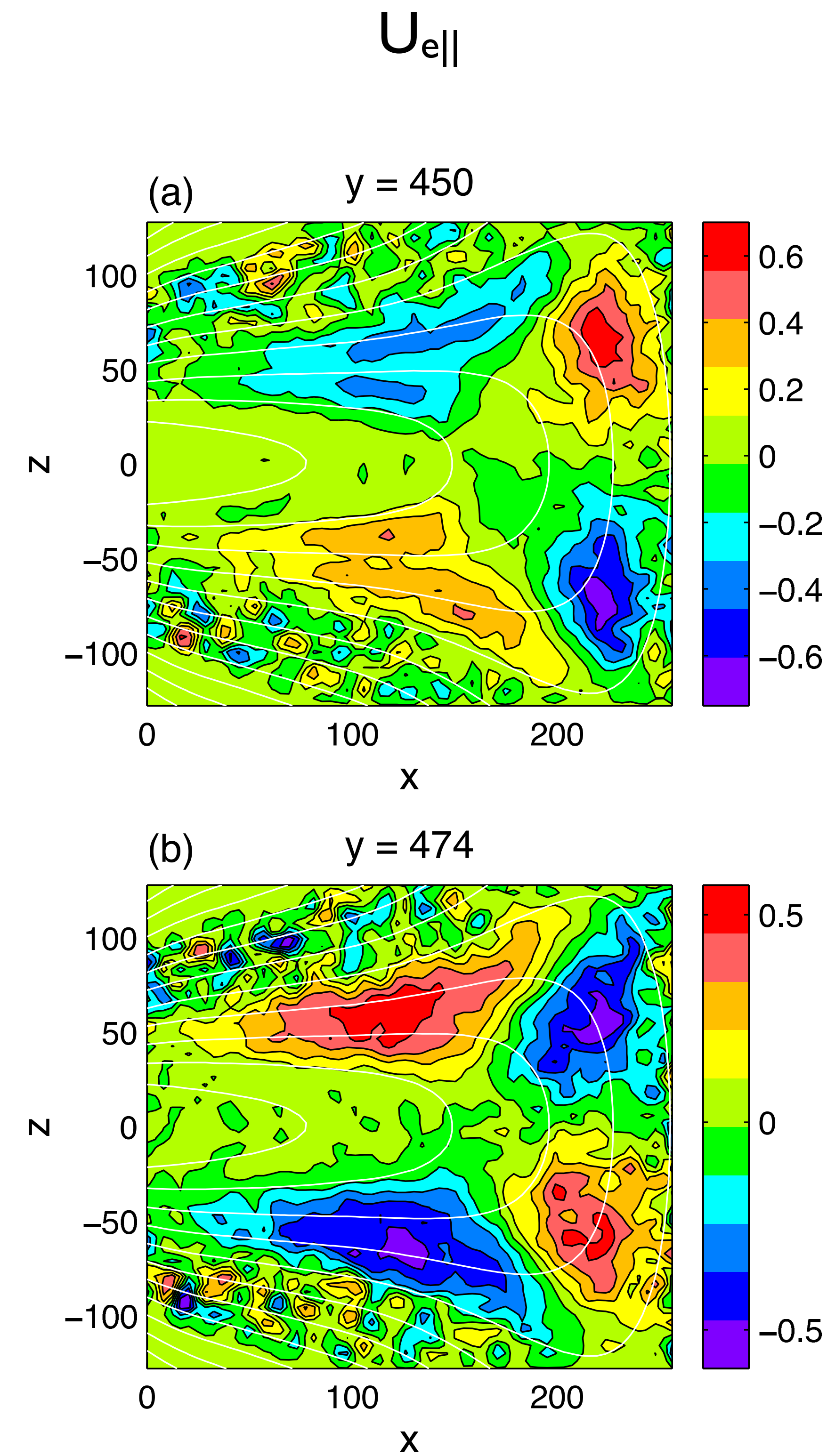

Initial case: $k_y\rho_{in}$ ~ 6

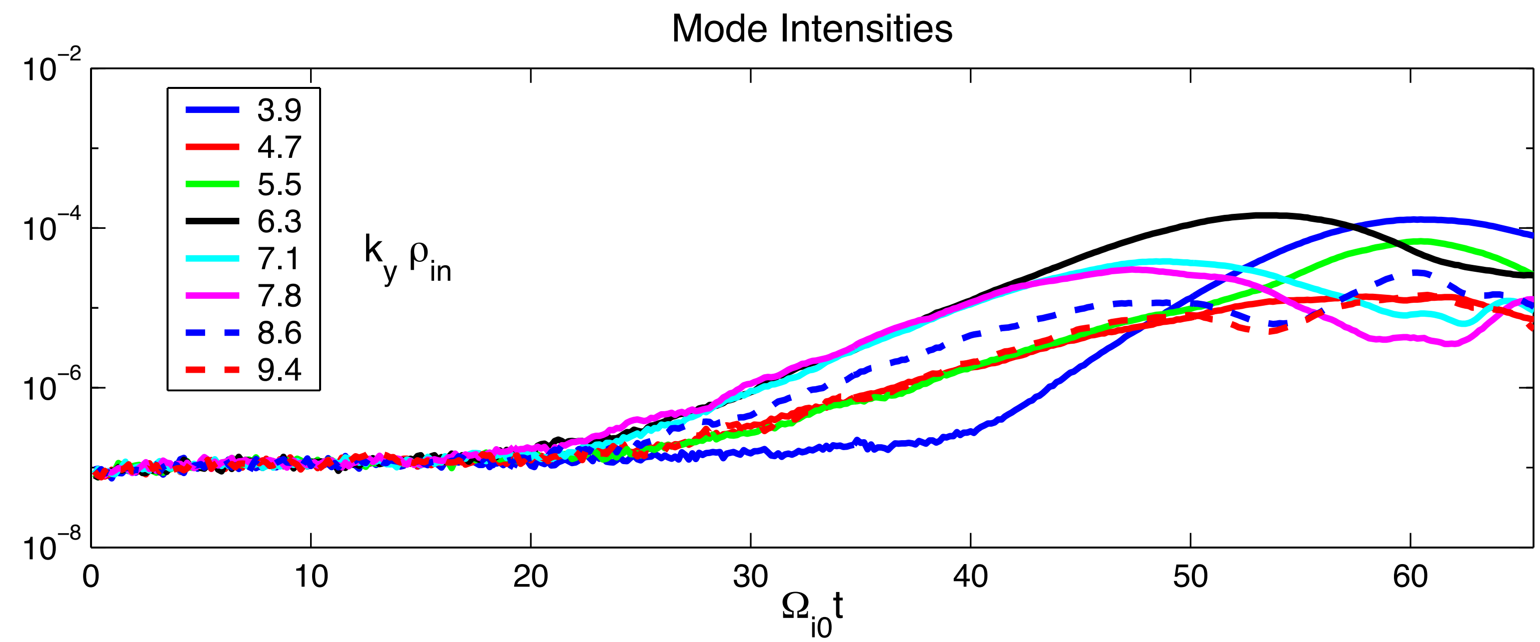

Second case: $k_y\rho_{in}$ ~ 1

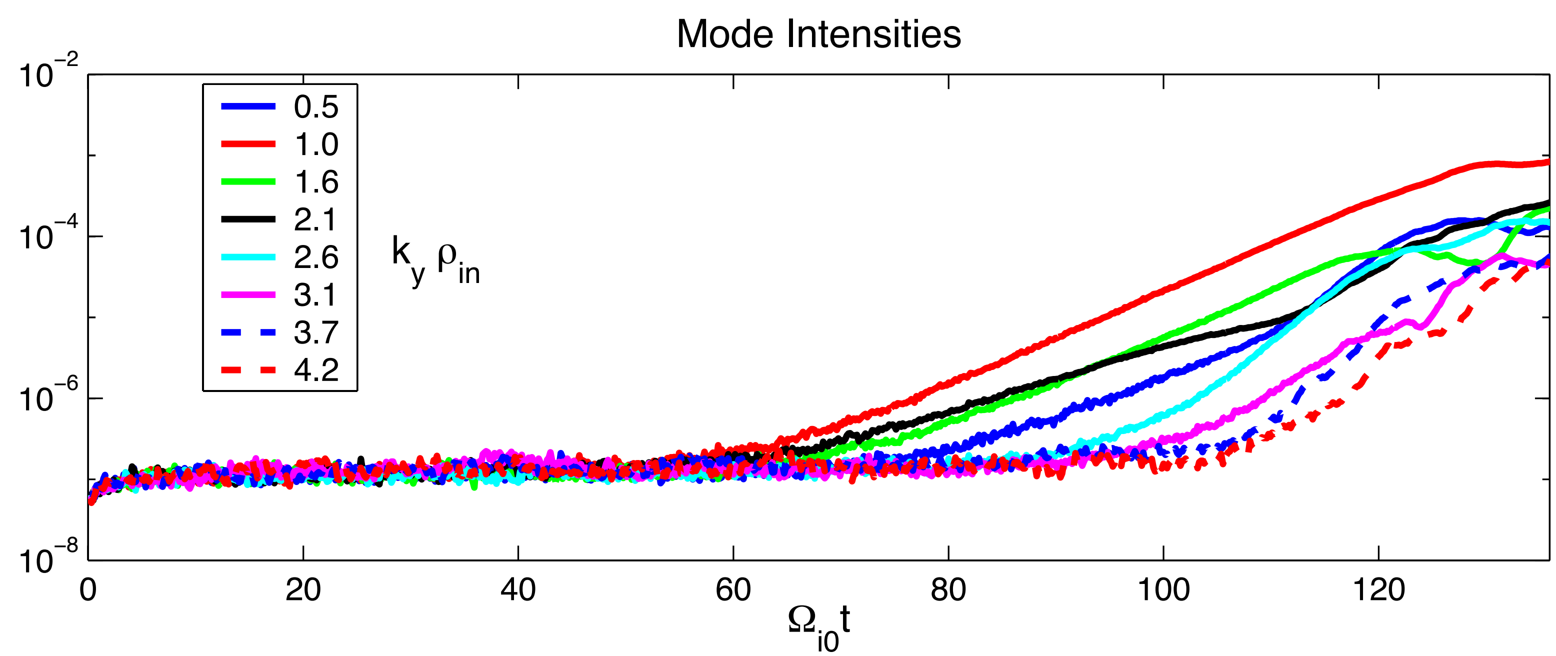

Mode Identification

- Consider linear kinetic analysis where we model $\delta\varphi$ and $\delta B_{||}$ along equilibrium field lines and compute the local ion and electron density perturbations at the midplane.
- Ions: Motion is stochastic (destroys gyromotion) and mode localized in x,z to ρ_{in} scale straight line orbits, respond only to electrostatic perturbation

$$\delta n_i/n_L = [Z'(s)/2]\, e\delta\varphi/T = -[1 + sZ(s)]\, e\delta\varphi/T, \qquad s = (\omega - k_y v_{di})/k_y v_{Ti}$$

$$\delta n_i/n_L = -[0.532 + 0.577i]\, e\delta\varphi/T$$

WRONG PHASE RELATION

Electron orbits average interaction with wave fields over flux tube volume; flux-tube averaged perturbed ion density becomes

$$\langle \delta n_i/n_L \rangle = -[0.75 + sZ(s)/2] = -[0.515 + 0.289i] e\delta\varphi_0/T$$

AGREES WITH SIMULATION

- Electrons: Electron orbits are adiabatic ($\kappa_e >> 1$) but wave and drift frequencies are not small compared with the bounce frequency. Thus full kinetic response including bounce and drift resonance interactions must be retained. Find that perturbed electron and ion flux tube averaged densities are in agreement.
- Perturbed densities yield dispersion relation consistent with the simulations. The dominant polarizations $\delta\varphi$ and $\delta B_{||}$ are similar to polarization of lower hybrid drift instability in straight magnetic field geometry; the present ballooning/interchange mode appears to be related to the low frequency limit of the LHDI.

Effect of Background Density on BICI

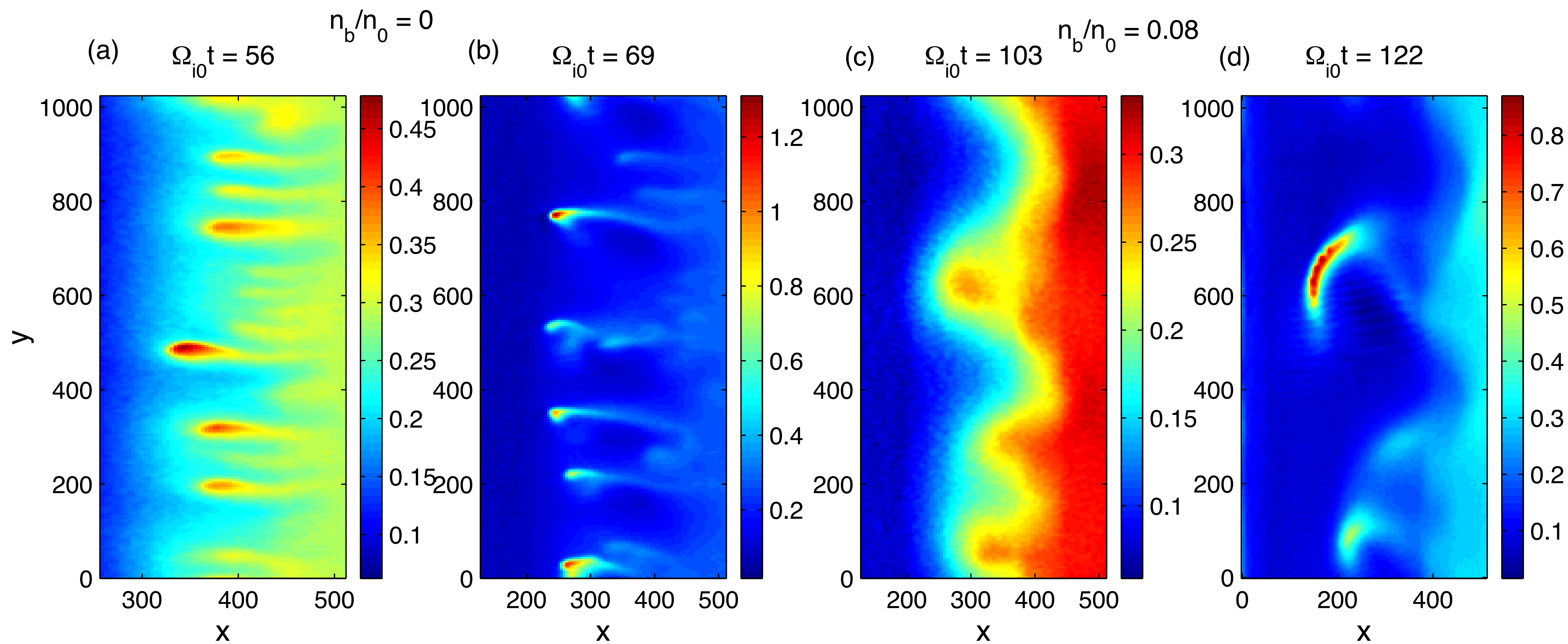

- Initial case ($n_b = 0$): linear BICI spectrum peaks at $k_y\rho_{in} \sim 6$ (wavelength ~ ρ_{in}); during earthward propagation, heads narrow and peak B_z increases, leaving several dominant heads with width ~ 600 - 900 km.

- Second case ($n_b/n_0 = 0.08$): peak wavenumber is much smaller ($k_y\rho_{in} \sim 1.0 - 1.5$). Nonlinear evolution produces single dominant head with width ~ 5000 - 6000 km. This is now compatible with observed scale of DFs.

Equatorial Plane DF Structure

- Transition thickness of B_z (from 0.25 to 0.80) occurs over distance of 11 Δ = 1.1 d_i.
- Density drops by factor of 3 across the front.
- E_y strength increases with B_z to a peak of ~ 11 mV/m
- Ion bulk flow speed increases only slowly across front and reaches max. behind the front ["growing" DF - Fu et al., 2011]
- Electron bulk flow exceeds the ion behind the front but is smaller ahead of front. Magnetic flux frozen in to electron flow ⇒ net increase in flux entering front as opposed to leaving ⇒ amplification of front.

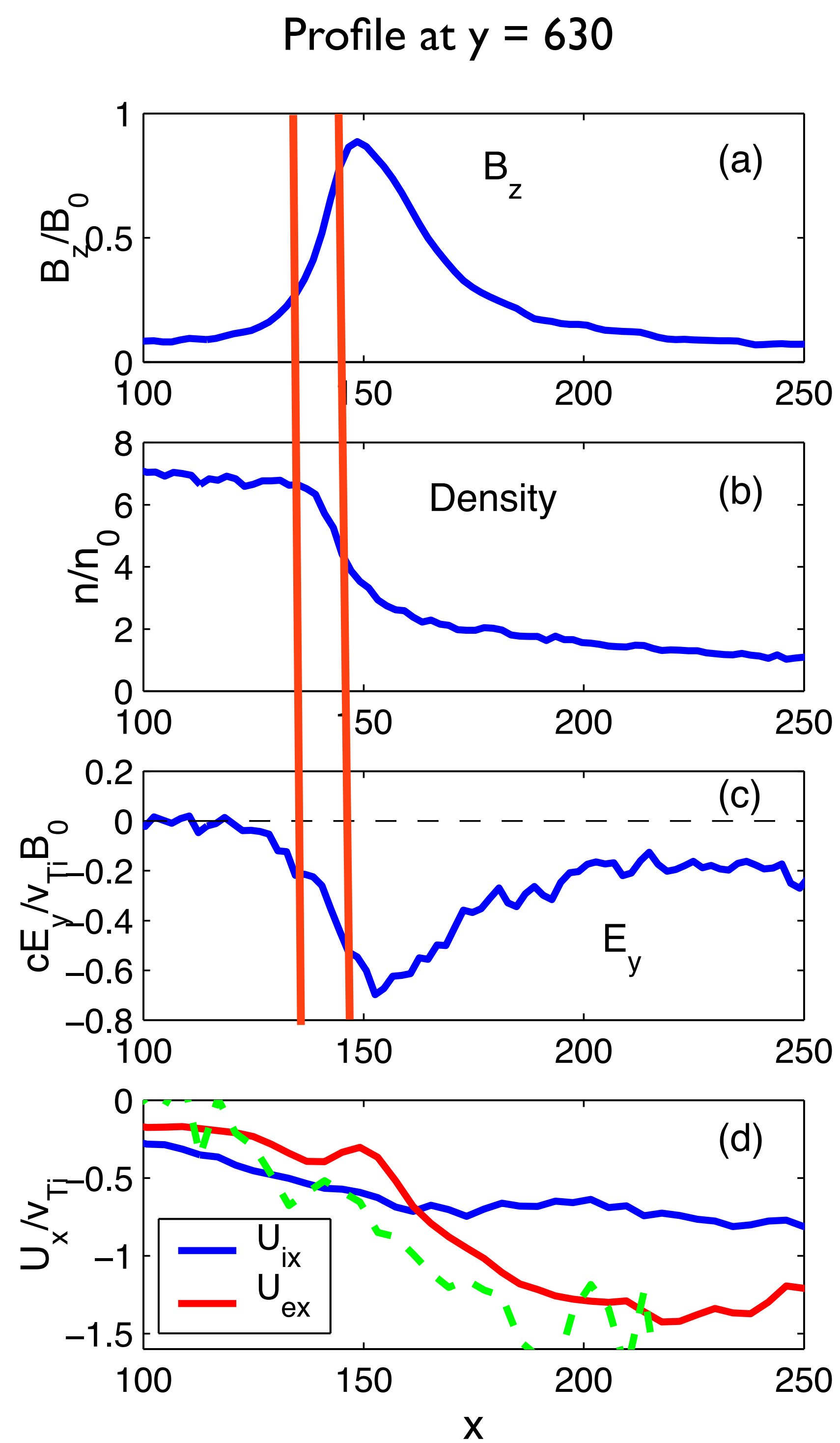

Breakup of DF Head and FACs

- As DF propagates earthward, B_z increases; breakup occurs when local ρ_{in} < DF thickness.
- Multiple sub-heads comparable to local gyroradius.
- Cross-tail current J_y diverted around each of the heads.
- Pair of Region I sense FACs associated with each subhead.
- FAC structuring of the DF is manifested in auroral streamer. A number of such structured streamers have been observed by THEMIS.

$\Omega_{i0}t = 127$

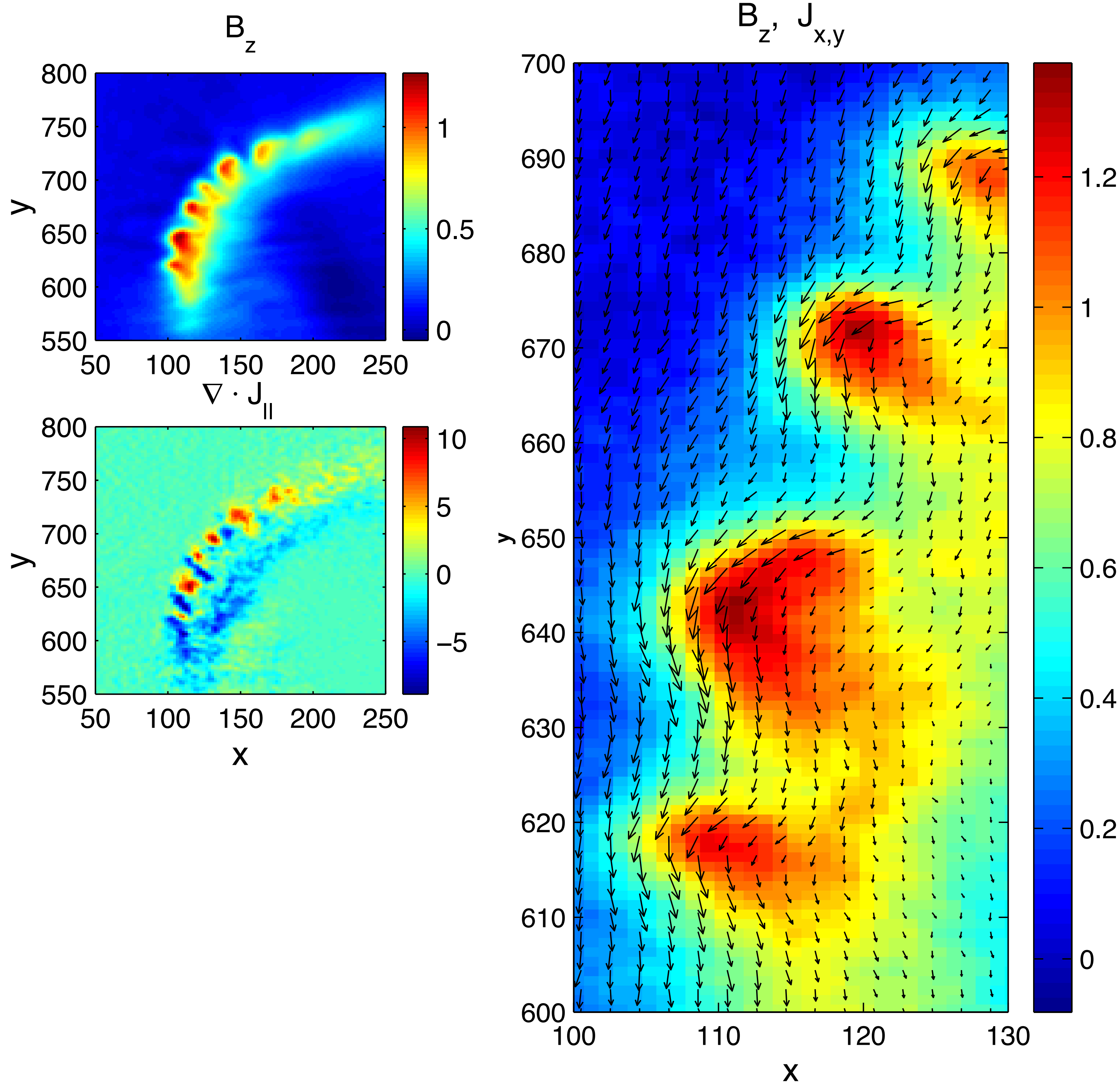

THEMIS ASI OBSERVATION

Structured Auroral Streamer

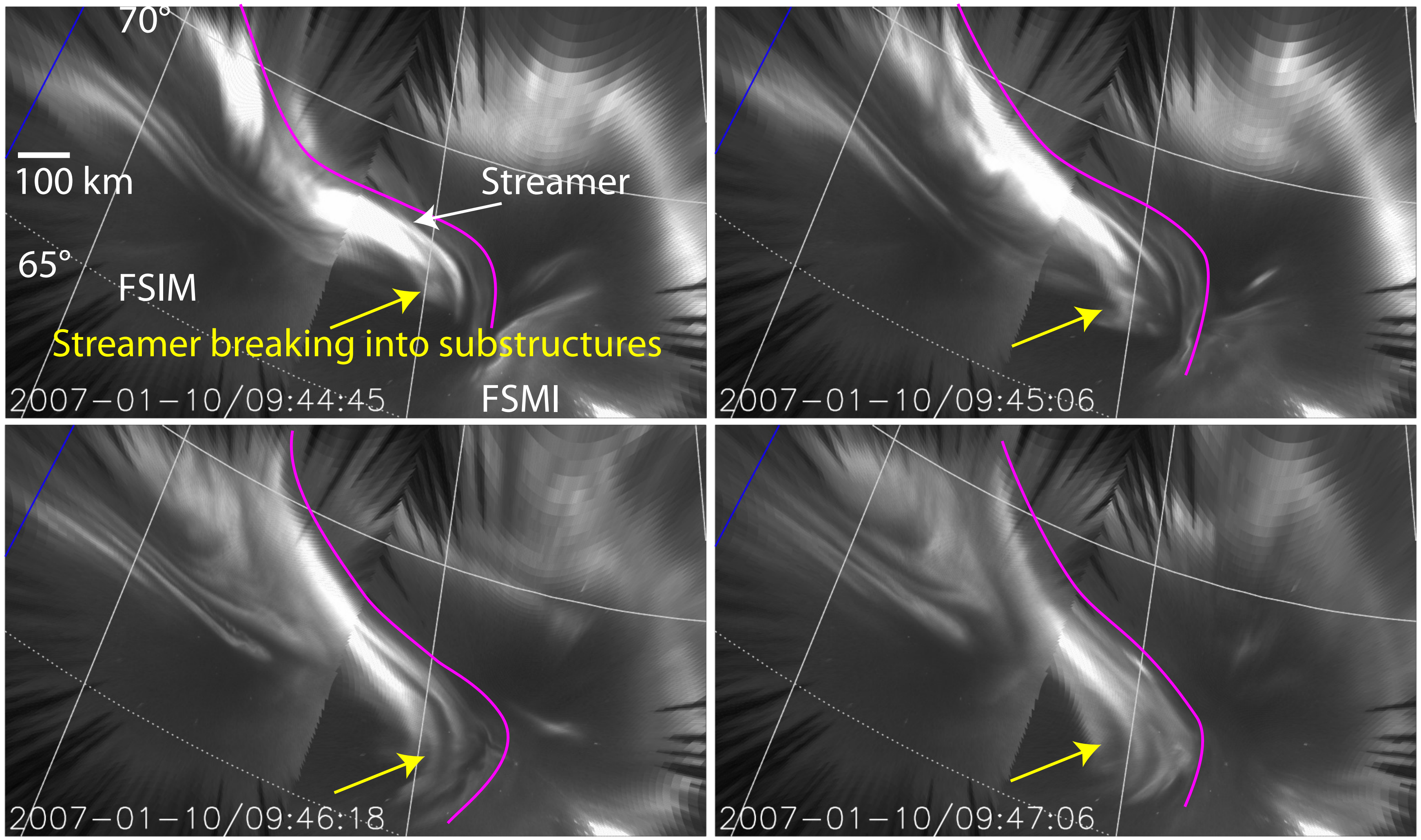

Size at 110 km:	substructure ~ 30 km	poleward portion ~ 100 km
Map to plasma sheet:	~ 1000 km width	~ 3000 km
Simulation:	subhead ~ 800 km	upward FAC region ~ 4000 km

Off-Axis Properties of DF at the edge of the density gradient

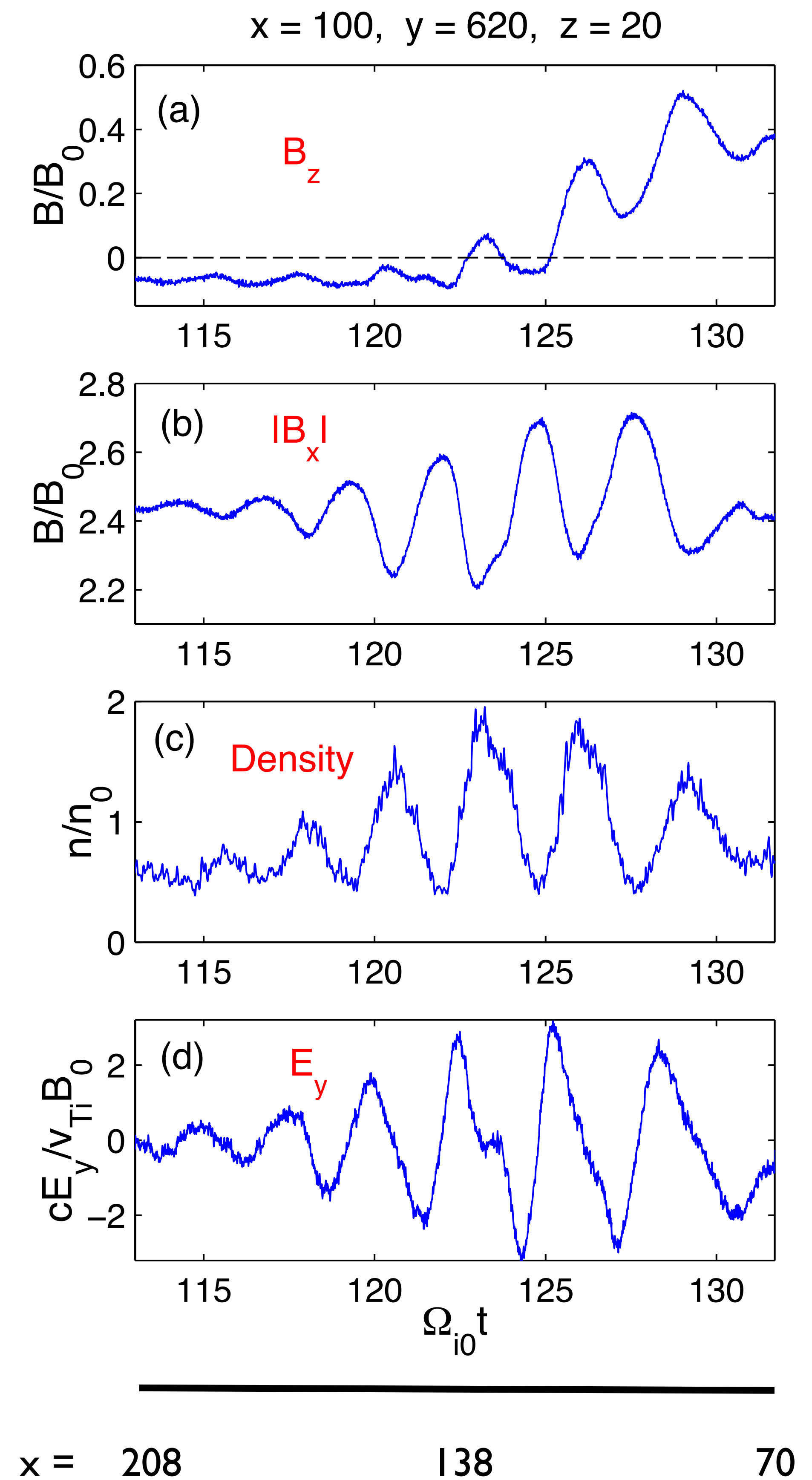

- Away from the center of the plasma sheet, the DF is strongly modulated in time in association with intense wave activity.
- This activity is a precursor to the actual arrival of the DF.
- The modulation is most apparent in E_y, B_x, and density, with less pronounced variation in B_z.
- $cE_y/V_{Ti}B_0$ = 2 - 3 or 30 - 50 mV/m.
- EM waves with $\delta E/\delta B \sim 4 V_A$.
- Similar intense waves much closer to the axis have been reported by M. Zhou et al. (2014), $B_z >> B_x$.

M. Zhou et al.   2014

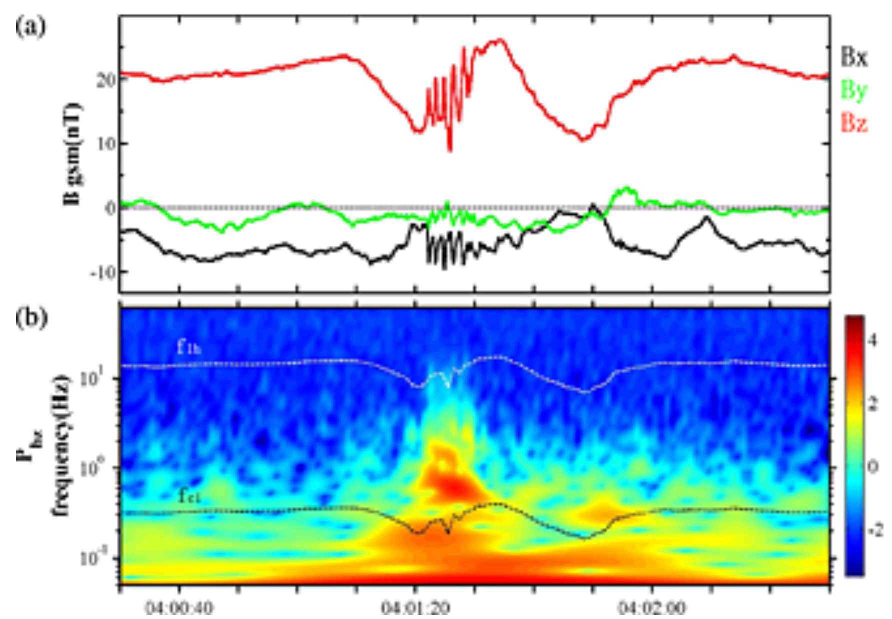

Intense EM Waves

- Wave activity concentrated in region of DF and extends somewhat duskward.
- Waves propagate duskward at 0.51 V_{Ti}
- Wavelength = 0.7 x (local d_i)
  = 700 km
- Frequency = 0.24 ω_{lh}
  = 0.96 $\Omega_{i,loc}$
- Standing wave structure along field lines

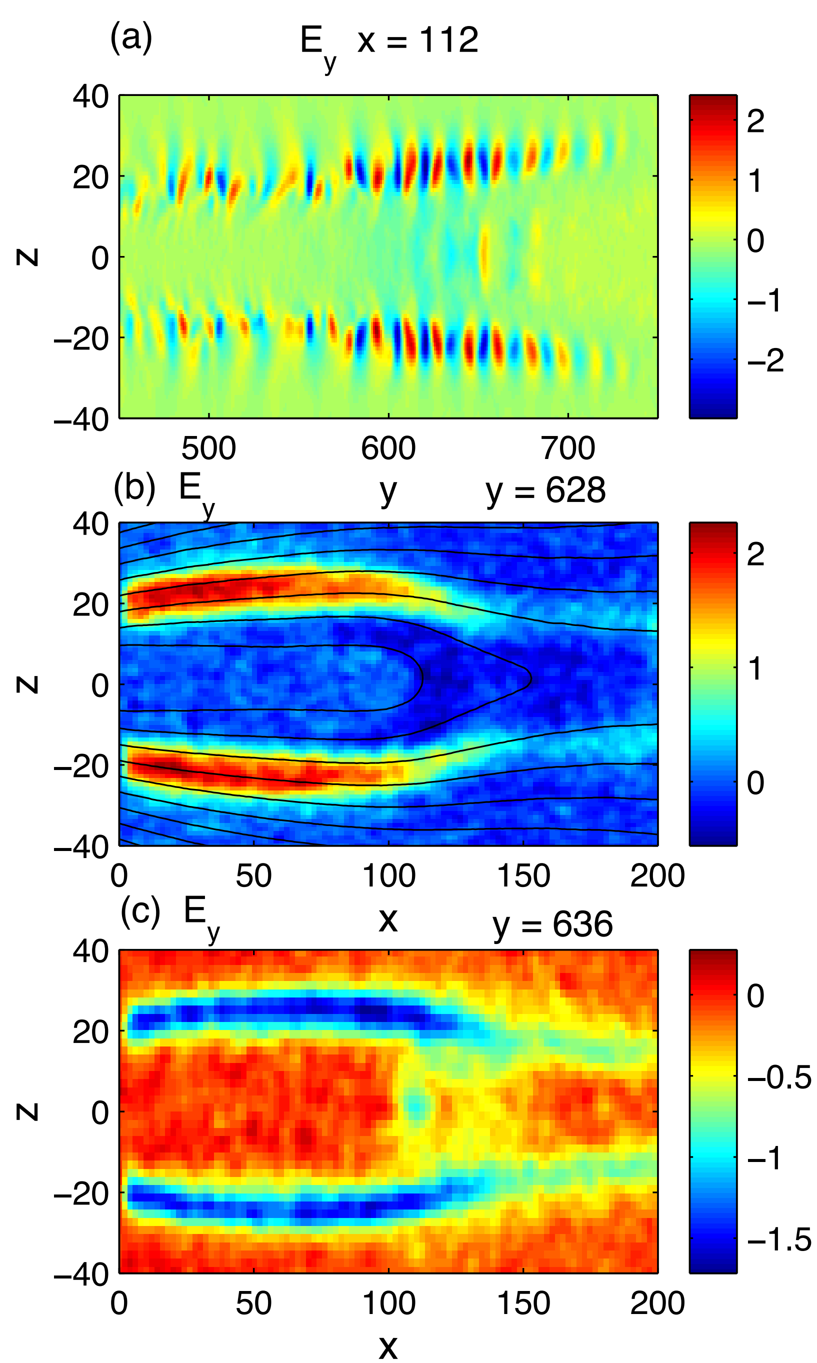

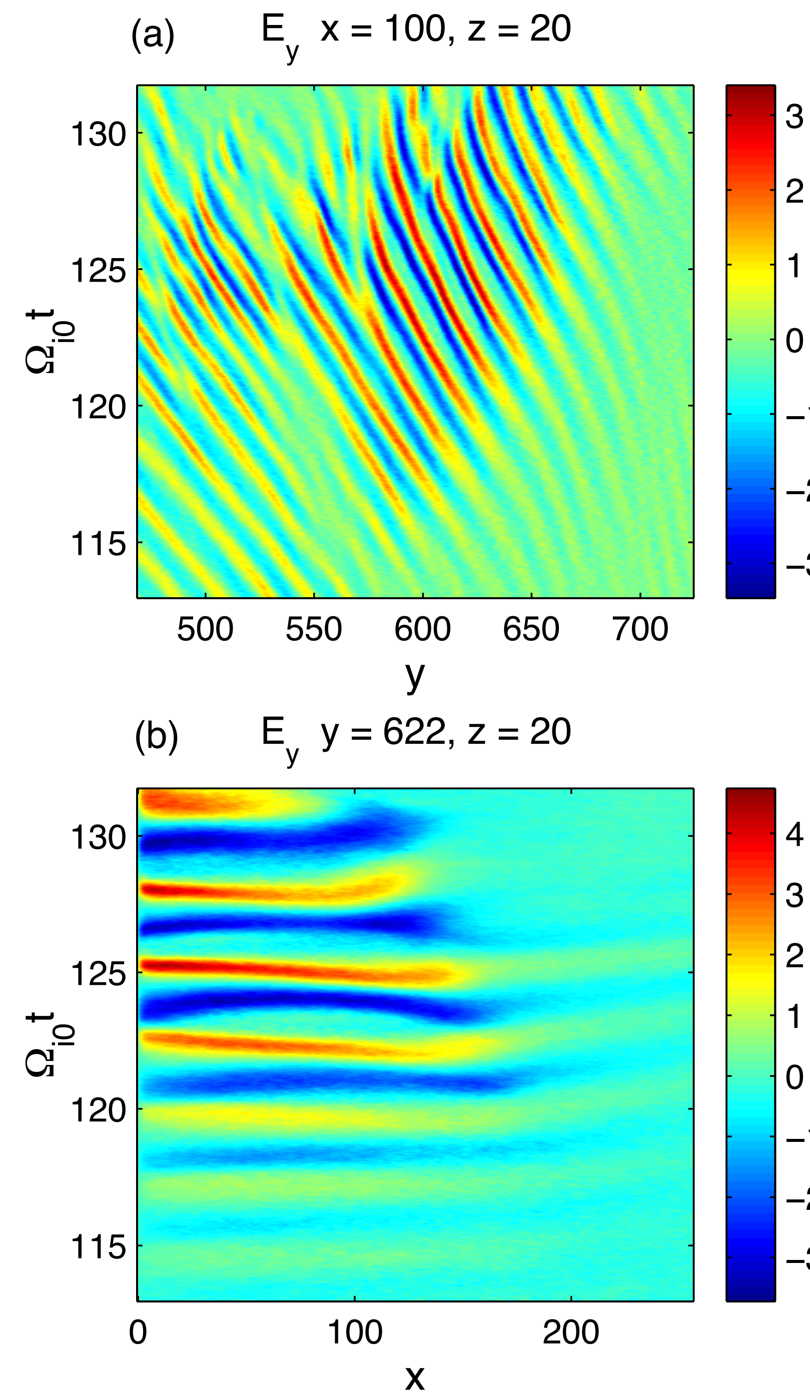

Particle Distributions in regions of intense waves
x = 110, z = -22

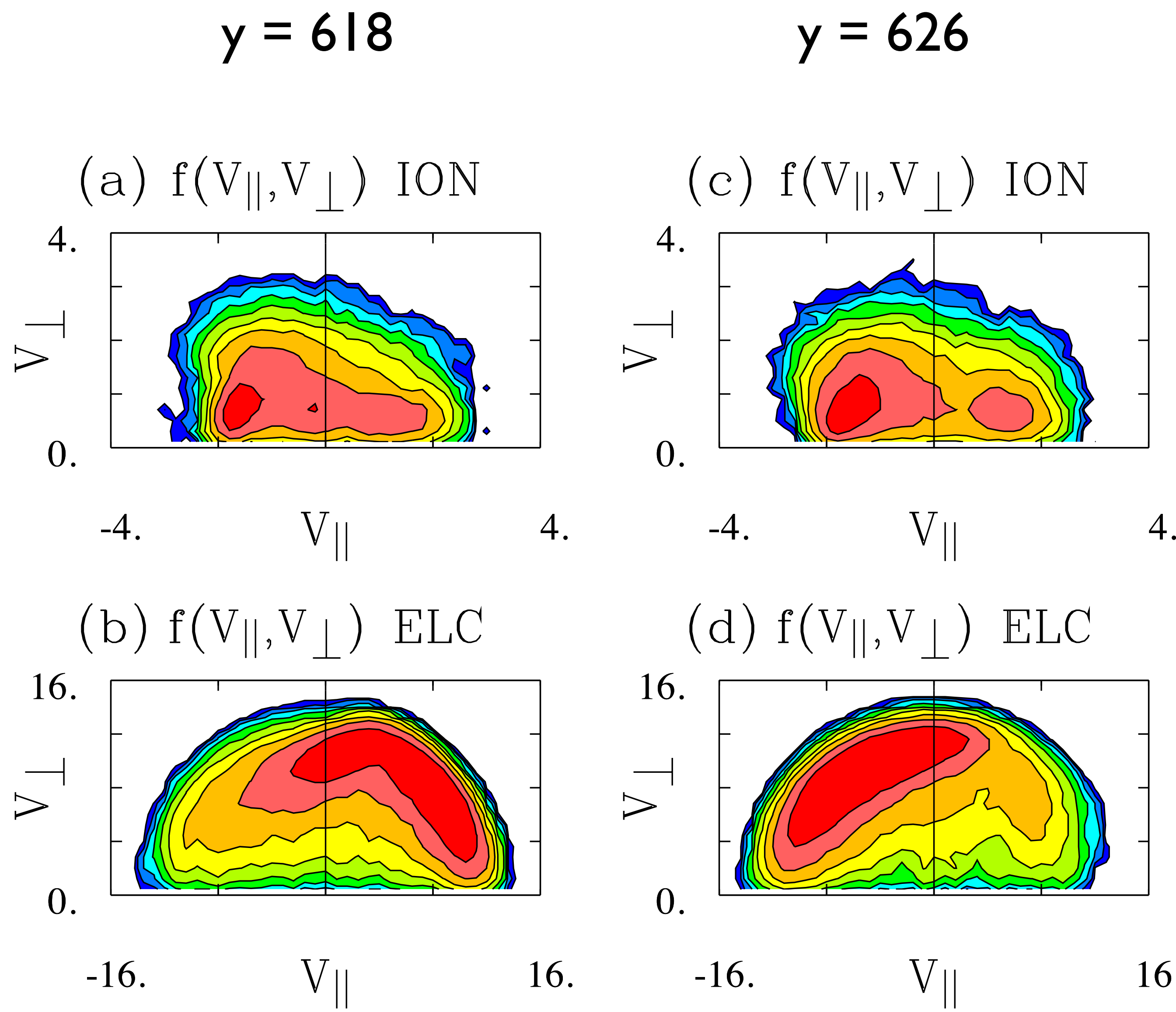

Large net parallel drift for electrons that reverses sign depending on wave phase; net ion - electron parallel drift ~ 3.5 V_{Ti}. Likely to drive electro-magnetic ion cyclotron instability [Perraut et al., 2000].

Zhou et al. (2014) attribute waves to $\partial f_i/\partial v_\perp > 0$ and identify it as ion Bernstein.

Also strong $\partial f_e/\partial v_\perp > 0$ slope ⇒ electron cyclotron harmonic waves.

Dissipation

- In wave region alternating regions of generator ($E \cdot J < 0$) and load ($E \cdot J > 0$); very little dissipation ($E' \cdot J > 0$), where $E' = E + U \times B$.

- Strong dissipation is localized (on slightly sub-d_i scale) at the sub heads of the DF, $E' \cdot J \sim 2$ nW/m^3.

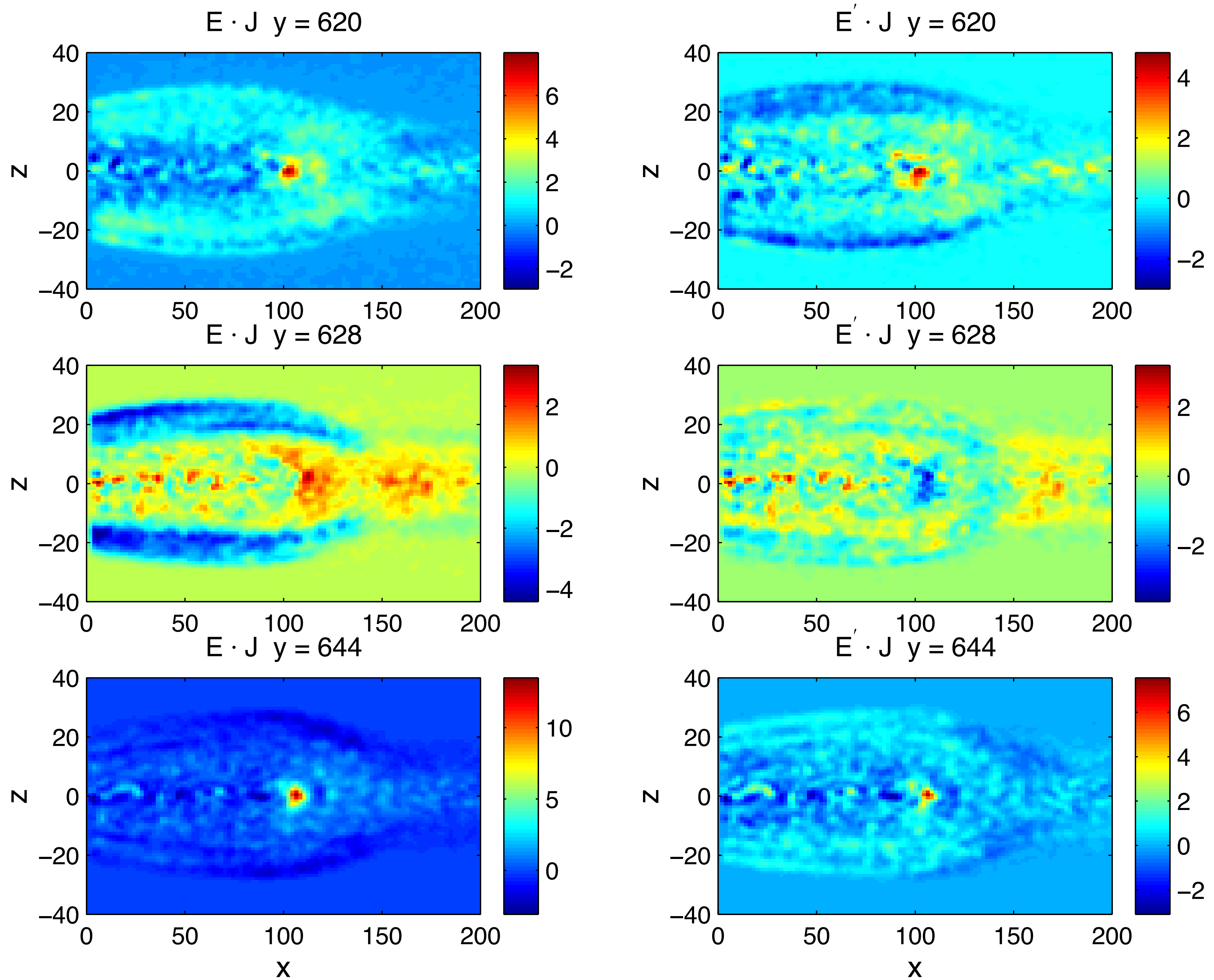

Poynting Vector Components

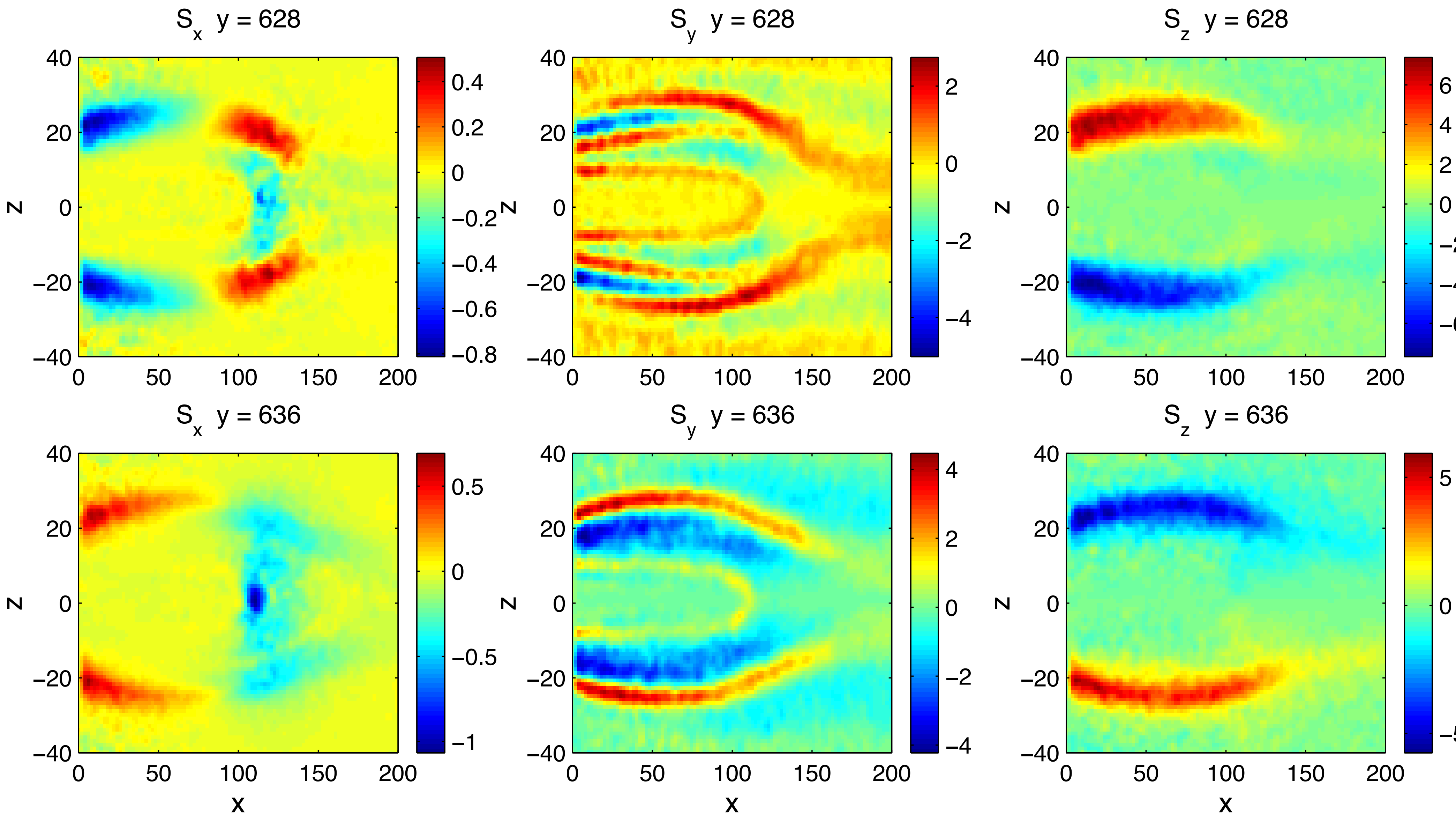

Intense Poynting Vector Fluxes:

- Circulating cell patterns (north-dawn-south-dusk) ~ 1 mW/m^2
- Alternating components to and from ionosphere ~ 0.1 mW/m^2

Properties of Reconnection Fronts

- Multi-point studies suggest that full width of high-speed flow channels in plasma sheet are of order 1 - 3 R_E (Sergeev et al., 1996; R. Nakamura et al., 2004).

- Can such finite cross-tail flows be produced directly by reconnection?

- Hall MHD studies indicate that expansion of a finite reconnection region proceeds at a rate given by the relative electron - ion flow speed (Huba and Rudakov, 2002; Shay et al., 2003; TKM Nakamura et al., 2012).

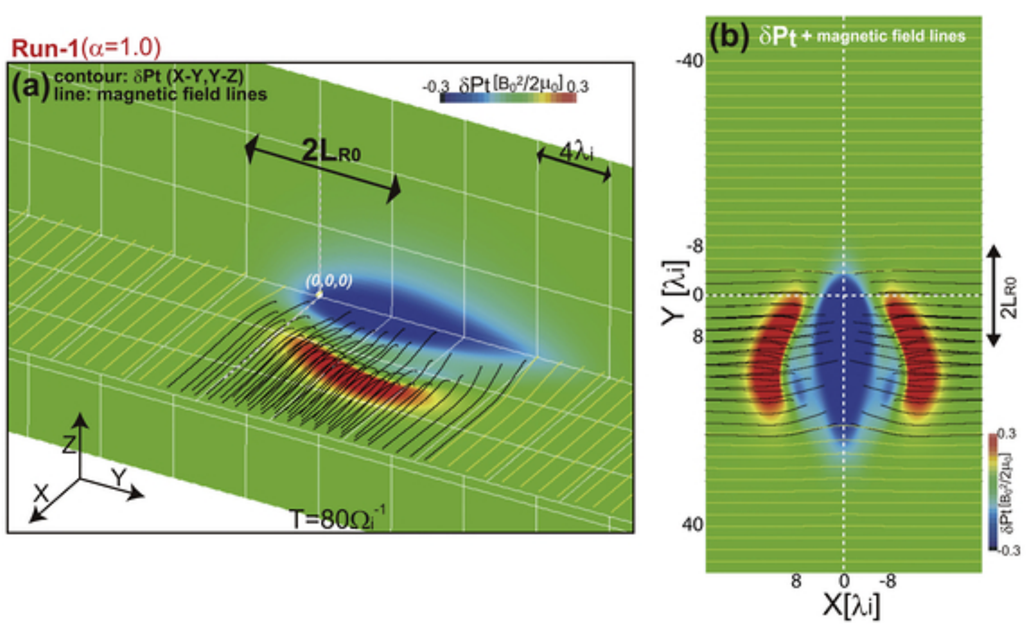

Ions carry initial current

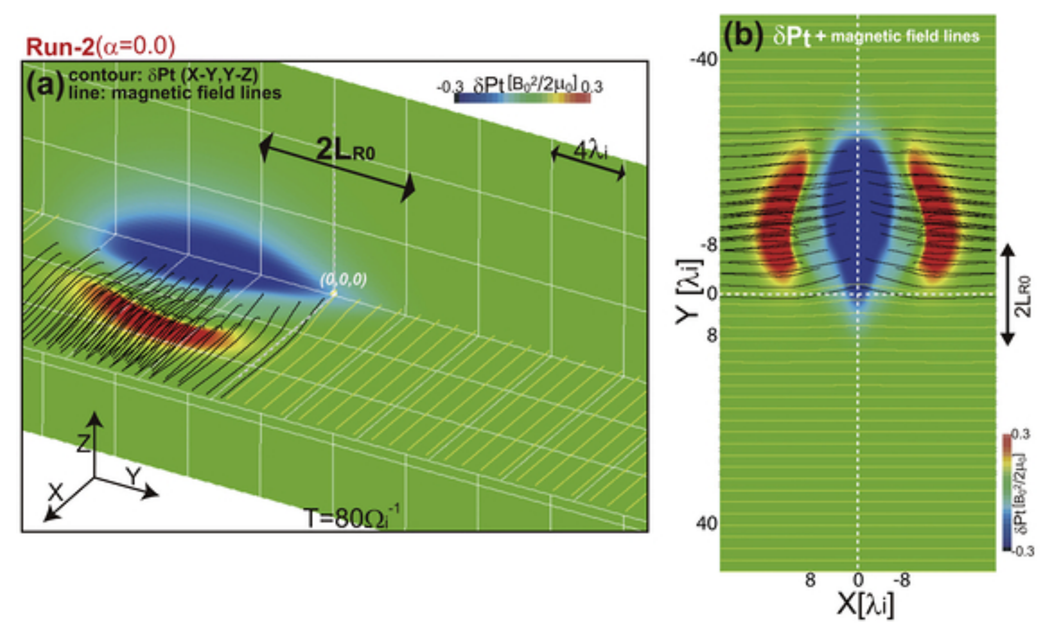

Electrons carry initial current

- Use 3D PIC simulation in which localized region is initiated by periodically blocking the J_y current density in the center of the current sheet (Pritchett & Coroniti, 2002). This represents the upper limit to the effects that can be produced by the onset of an anomalous resistance within a growth phase thin near-Earth current sheet. The blocking leads to an enhancement of the E_y and to the formation of a localized reconnection region.

- Initial blocking region: $0 < x < 3d_i$, $30d_i < y < 34d_i$

- System size: $-64d_i < x < 64d_i$, $0 < y < 64d_i$

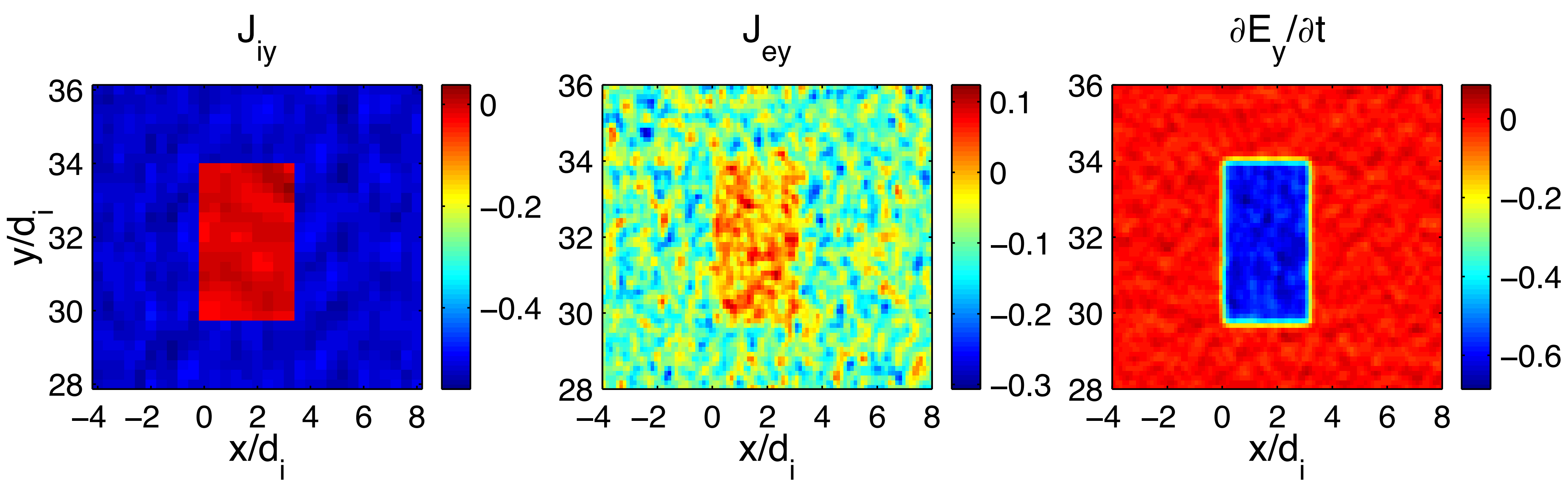

- Max B_z follows electrons slightly dawnward, but the jet front is blown duskward by the ion flow; elongated front on scale of tens of d_i >> initial perturbation.

- Extended front appears to break up on scales of a few d_i.

Add 0.02 normal field and vary width of blocking region.

- Breakup less pronounced on tailward propagating front.

- Appears likely to have a minimum width of front.

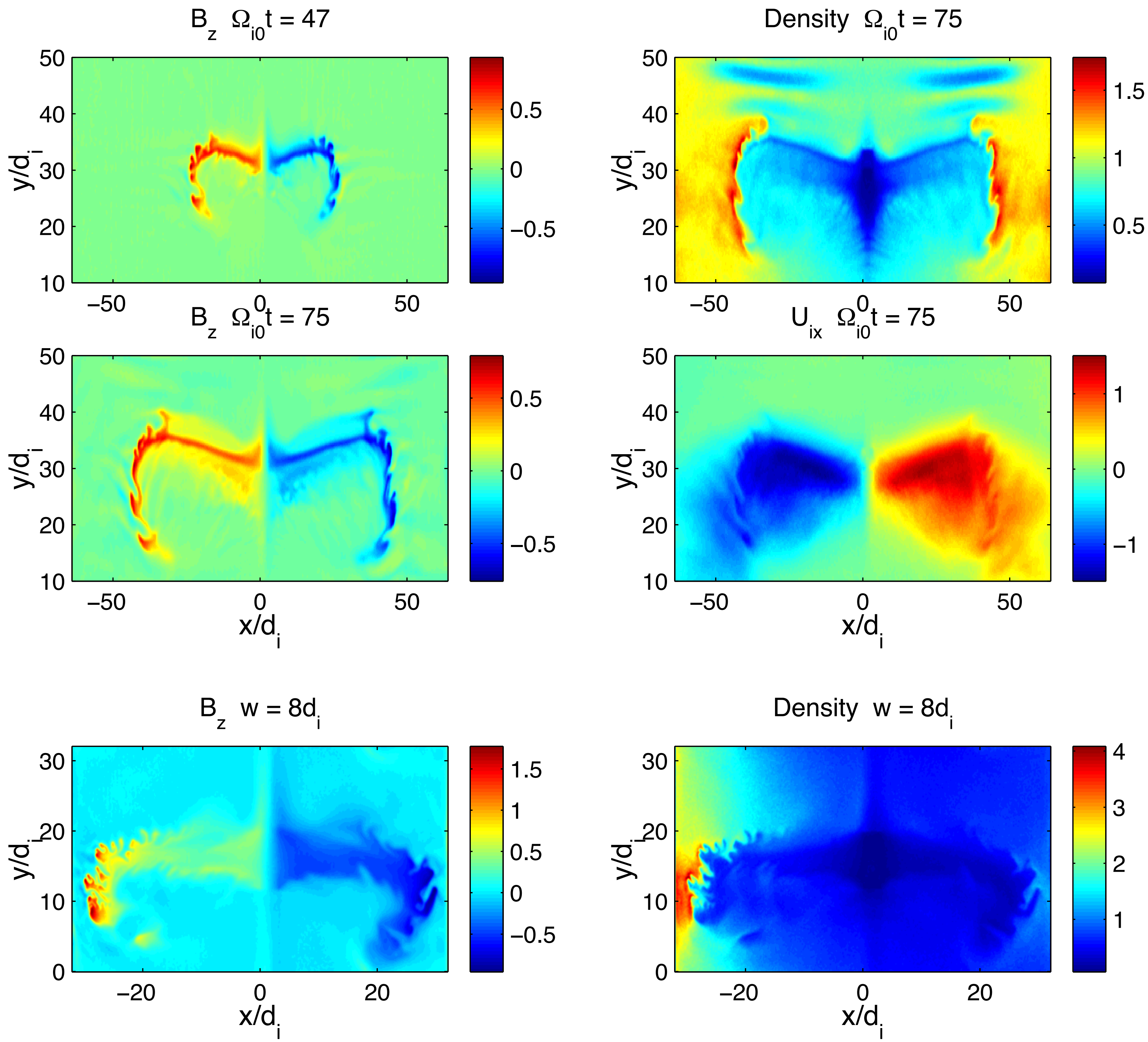

Summary/Questions

- Key feature of plasma sheet is presence of a finite B_z component. This necessitates a kinetic treatment of plasma sheet dynamics.

- Spontaneous tearing instability appears to be unlikely due to magnetization of the electrons. How can reconnection be initiated?

- Jet (dipolarization) fronts are common feature of the tail; possess kinetic scale thickness. What determines the cross-tail extent of ~ 1 - 3 R_E?

- Ballooning/interchange mode reproduces the key features of the fronts and predicts the structuring of auroral steamers and the presence of intense off-axis EM waves near Ω_{ci}. Recent THEMIS observations offer confirmatory examples of these features.

- But how common are the conditions of decreasing entropy with radial distance down the tail that appear to be necessary for excitation of the modes?

- Can localized perturbations (perhaps from the dayside) produce reconnection jets that mimic the properties of the BICI mode?

- What happens when these fronts impact a growth-phase thinned near-Earth plasma sheet system?